IEEE Access
Multidisciplinary | Rapid Review | Open Access Journal

Received 16 January 2025, accepted 1 February 2025, date of publication 5 February 2025, date of current version 20 February 2025.

Digital Object Identifier 10.1109/ACCESS.2025.3539572

TOPICAL REVIEW

Review of Cryogenic Power Electronics for All-Electric Aircraft

ABDELRAHMAN ELWAKEEL, (Member, IEEE), YUCHUAN LIAO, (Graduate Student Member, IEEE), YUDI XIAO, (Member, IEEE), RAFAEL PEÑA ALZOLA, (Senior Member, IEEE), MIN ZHANG, (Senior Member, IEEE), AND WEIJIA YUAN, (Senior Member, IEEE)

Department of Electronic and Electrical Engineering, University of Strathclyde, G1 1XQ Glasgow, U.K.

Corresponding author: Abdelrahman Elwakeel (Abdelrahman.elwakeel@strath.ac.uk)

This work was supported by UKRI and by the EPSRC under grant EP/Y006437/1.

ABSTRACT To tackle emissions from the aviation industry and make it sustainable, research has been targeting electrifying aircraft. For this aim, articles have been focusing on how to replace regular jet engines with liquid hydrogen as fuel. This would be beneficial as hydrogen is expected to play a dual role, providing fuel for fuel cells to propel the aircraft electrically and to supply cooling to enable high-power density technologies such as superconducting machines and cryogenic power electronics circuits. However, using higher power density, especially cryogenic power electronics, can be challenging. This article investigates cryogenic power electronics for use on all-electric aircraft across different aspects, where it lays out how to integrate power electronics at cryogenic temperature into the architecture of the all-electric aircraft, how to use them with hydrogen fuel cells, and the voltage levels of the system. It reviews different semiconductor device technologies, circuit topologies, and passive devices to be used in power electronics circuitry, as well as logic circuits that are suitable for use at cryogenic temperatures. In addition, the article discusses the challenges of using semiconductor devices at such low temperatures, including the reliability, overall cooling, and recycling of hydrogen.

INDEX TERMS Cryogenic electronics, gate driver, IGBT, MOSFET, cryogenic propulsion.

ACRONYMS

AC	Alternating current.
ANPC	active neutral point clamped.
C	Celsius.
CO2	Carbon dioxide.
COTS	Commercials off the shelf devices.
CMOS	Complementary metal oxide semiconductor.
COP	Coefficient of performance.
DAB	Dual active bridge.
DC	Direct current.
DCB	Direct bonded copper.
DCCT	DC current transformer.
DPT	Double pulse test.
DUT	Device under test.
ECS	Environmental control system.
EMA	Electromechanical actuators.
EHA	Electro-hydraulic actuators.
GaN	Gallium nitride.
GH2	Gaseous hydrogen.
H2	Hydrogen.
HBLLC	Half bridge LLC.
HEMT	High-electron-mobility-transistor.
HTS	High –temperature superconductors.
HV	High voltage.
IC	Integrated circuit.
IGBT	Insulated gate bipolar transistor.
JFET	Junction field effect transistor.
K	Kelvin.
kg	kilogram.
kW	kilo-watts.
kV	kilo Volt.
LH2	Liquid hydrogen.

The associate editor coordinating the review of this manuscript and approving it for publication was Alexander Micallef.

LN2	Liquid nitrogen.
MEA	More electric aircraft.
MIL-STD	Military standard.
MLI	Multi-layer insulation.
MOSFET	Metal-oxide-semiconductor-field-effect-transistor.
MMC	Modular-multilevel converter.
mW	milli-watt.
MW	mega-watt.
NASA	National Aeronautics and Space Administration.
NPC	neutral point clamped converter.
PCB	printed circuit board.
PD	partial discharge.
PWM	Pulse width modulation.
PSU	power supply unit.
Si	Silicon.
SiC	silicon carbide.
SC-PWM	Shifted carrier PWM.
SiGE	Silicon germanium.
SLC	Solid cover.
SFCL	superconductor fault current limiter.
WBG	wide-bandgap.
UFS	ultrafast switch.
ZCS	zero current switching.
ZVS	zero voltage switching.

I. INTRODUCTION

All Electric Aircraft has been the main focus of research as countries are planning to reduce emissions from the aviation industry which accounts for 2.5% of the global CO_2 emissions [1]. Companies and governmental organizations such as Airbus, Rolls-Royce, and NASA have been investing in researching fully-electric commercial aircraft [2], [3], [4]. Currently, Airbus is aiming to have a commercial fully electric aircraft by 2035 employing hydrogen as an energy source. Hydrogen can also be a key enabler for cryogenic propulsion which utilizes technologies such as superconducting motors and cryogenic power electronics, which are known to have higher power density and higher efficiency than their room temperature counterparts. In this article, cryogenic temperatures would be referred to if the temperature is below 123 K. Such extreme conditions are crucial for enhancing the efficiency and power density of the aircraft's electrical systems, paving the way for practical, long-range electric flight. With high power densities, cryogenic power electronics and superconducting machines can pave the way for aircraft electrification, this is shown when a comparison is made between the current energy density of a B737 is around 12 kW/kg whereas in all-electric aircraft, the targeted energy density is above 20 kW/kg for cryogenic power electronics and above 35 kW/kg for superconducting machines [5].

There are different types of all-electric aircraft, those using batteries as the energy source, and those using hydrogen turbines or fuel cells. Although even the most optimistic projections predict that this will reach 500 Wh/kg by 2030, single-aisle size aircraft viability requires a battery pack-specific energy of at least 800 Wh/kg when considering the option of full electrification. For large commercial aircraft, where energy density is critical, cryogenic propulsion is a suitable choice to realize such a vision. The architecture of all-electric aircraft that utilizes cryogenic propulsion is based on the literature [5], [6], [7], where superconducting motors and cables are expected to be used due to their high-power density when compared to machines and cables that utilize copper or aluminum conductors. The superconducting motors and cables are expected to be cooled down to 20K. Power electronics circuits are also expected to work at cryogenic temperature and this is better from an engineering point (better thermal design) with the entire system working in the same temperature region. It is expected that power electronics will work at a temperature higher than 100K to prevent carrier freezeout.

Even though many review articles have discussed all-electric aircraft and cryogenic power electronics, there is still some gap that needs be addressed. For example [5] and [6] have discussed the architecture of a cryogenic propulsion aircraft, however, which zones and applications of the aircraft are suited for cryogenic power electronics and which are suited for ambient temperature power electronics. Another review article [8], has only reviewed the performance of cryogenic power electronic devices without reviewing gate drivers and discussing the available commercial of the shelf device ratings. In [9], a brief review has been done on converter and inverter topologies however, that review was only top level and did not review more complex circuitry such as modular multilevel LLC or which inverter topology would have the highest power density and would be most effective to use on an electric aircraft. This paper has reviewed the device reliability and the type of testing that is important to determine the ruggedness of power electronic devices at cryogenic temperatures. To address these gaps this article reviews and investigates cryogenic power electronics and their suitability for achieving cryogenic propulsion in all-electric aircraft. The focus is on power electronic circuits tailored for such aircraft and how cryogenic technology can enhance efficiency and power density, building on previous work by the authors [10], [11], [12], [13], [14], and [15]. By examining device and circuit performance at cryogenic temperatures, the study aims to identify the benefits and challenges, providing insights into their practical implications for aircraft design and operation.

The article is divided into the following sections: Section II includes a top-level review of the electrical system distribution and drives. Section III will review the performance of semiconductor devices at cryogenic temperatures. Section IV reviews the performance of passive devices at cryogenic temperatures, Section V reviews the performance of power electronics circuits at cryogenic temperatures, Section VI reviews the performance of logic circuits at cryogenic temperatures, Section VII reviews cryogenic gate drivers for semiconductor switches and Section VIII reviews the current sensing circuits

at cryogenic temperatures. Section IX reviews the electrical distribution system in an electric aircraft, Section X reviews the challenges facing the transformation to a fully electric aircraft. Finally, Section XI includes the discussion and the conclusion of the article.

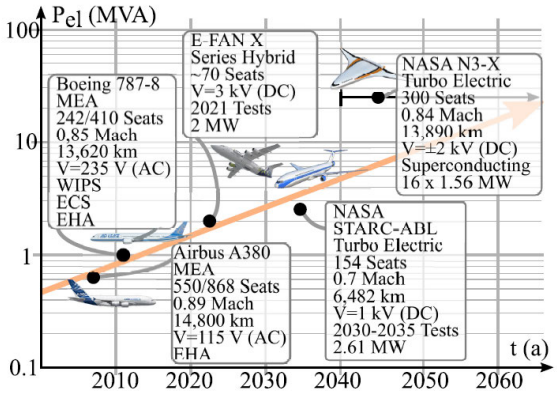

FIGURE 1. Electrification of aircraft [9].

II. ARCHITECTURE OF CRYOGENIC PROPULSION FOR ALL-ELECTRIC AIRCRAFT

In recent years, there has been a notable surge in projects for aircraft electrification, this is shown in Figure 1. The generated electric power has increased from several hundred kVA to currently 1 MW on flagship aircraft models such as the Boeing 787 and Airbus A380. In the coming years, as aircraft are being transformed to fully electric, forecasts predict a remarkable soar in the demand for electric power aboard flights. For example, it is predicted that a full-electric aircraft designed by NASA the N3-X will have a power of 25 MW.

A. ELECTRICAL SUPPLY FOR CRYOGENIC PROPULSION

Hydrogen is a key disruptor for the aviation industry as it has significantly higher gravimetric power density than batteries and traditional kerosene-based solutions. Hydrogen can reach a power density of 39.4 kWh/kg at the higher heating value of hydrogen compared with 11.9 kWh/kg for jet engine fuel [6], [9]. The high gravimetric power density of hydrogen implies that for a given weight, hydrogen can store and deliver much more energy than traditional jet fuel. This characteristic is particularly advantageous in aviation, where weight is a critical factor affecting fuel efficiency, range, and payload.

The primary drawback of using liquid hydrogen (LH2) compared to kerosene is its significantly larger volume requirement. Unlike kerosene, which has a higher energy density and therefore requires less storage space, liquid hydrogen needs at least four times the volume for equivalent energy output. Moreover, when comparing LH2 to GH2, the storage tanks for LH2 can be considerably lighter. This is because LH2 is stored at cryogenic temperatures, significantly reducing the pressure requirements for containment compared to gaseous hydrogen storage. References [7] and [16] how hydrogen can be integrated into the aircraft.

Nevertheless, transitioning to LH2 as a fuel source would necessitate modifications to the airframe and fuselage of aircraft. LH2's cryogenic nature requires specialized storage and handling infrastructure, which may require design alterations to accommodate its unique characteristics. Currently, the aviation industry is actively exploring and developing tube-and-wing designs tailored for hydrogen-powered aircraft. These designs aim to optimize the integration of LH2 storage systems, propulsion systems, and airframe structures to maximize efficiency and performance while meeting safety and regulatory requirements.

B. CRYOGENIC POWER ELECTRONICS

For cryogenic propulsion, the superconducting machine would require to be cooled to lower temperatures where hydrogen would be used as coolant. As the coolant would need to be already present for cryogenic propulsion, it would be better from a thermal point (lower thermal leakage) to have the power electronics system of the aircraft at the same temperature. In addition to providing easiness from the mechanical point of view, using power electronics at cryogenic temperatures would enable them to work more efficiently, have lower on-resistance, and have faster switching [6], [7], [8], [9], [10], [11], [12], [13], [14], [15]. An efficiency comparison is done between room and cryogenic temperature power electronics, where it is expected that efficiency would improve by 1.5% at lower temperatures rising from 98% to 99.5% [6]. Hence, in Figure 2, power electronics, motors, and superconducting cables are shown to work at lower temperatures.

C. ELECTRICAL SYSTEM STRUCTURE FOR CRYOGENIC PROPULSION

With the increase of the supplied power, a higher voltage is necessary to reduce the losses generated by the large amount of current supplied [9]. In compliance with standards there are specified voltage levels in MEA known in MIL-STD, which are explained below:

- DC voltage levels: 28 V, 270 V (±130 V), and 540 V (±270 V).
- 230 ph/115 ph V with variable frequency (e.g., 350-800 Hz in the B787), 230 ph V with fixed frequency (400 Hz), and 115 ph V with fixed frequency 400 Hz are the three AC voltage levels.

The main advantage of using 540 V is that the PD inception voltage would require less creepage distance [17].

Airports typically offer standardized voltage levels to accommodate maintenance requirements and ensure compatibility with components such as batteries and power electronics. For the E-Fan X project, Airbus proposed utilizing a voltage level of 3 kV. Initially, it was assumed that this voltage would be in the form of DC, which deviates from established standards such as MIL-STD–704 and DO–160 specifications. Currently, there is no official approved voltage rating for all-electric aircraft, and, to overcome that, the research and the industry have been focused on identifying

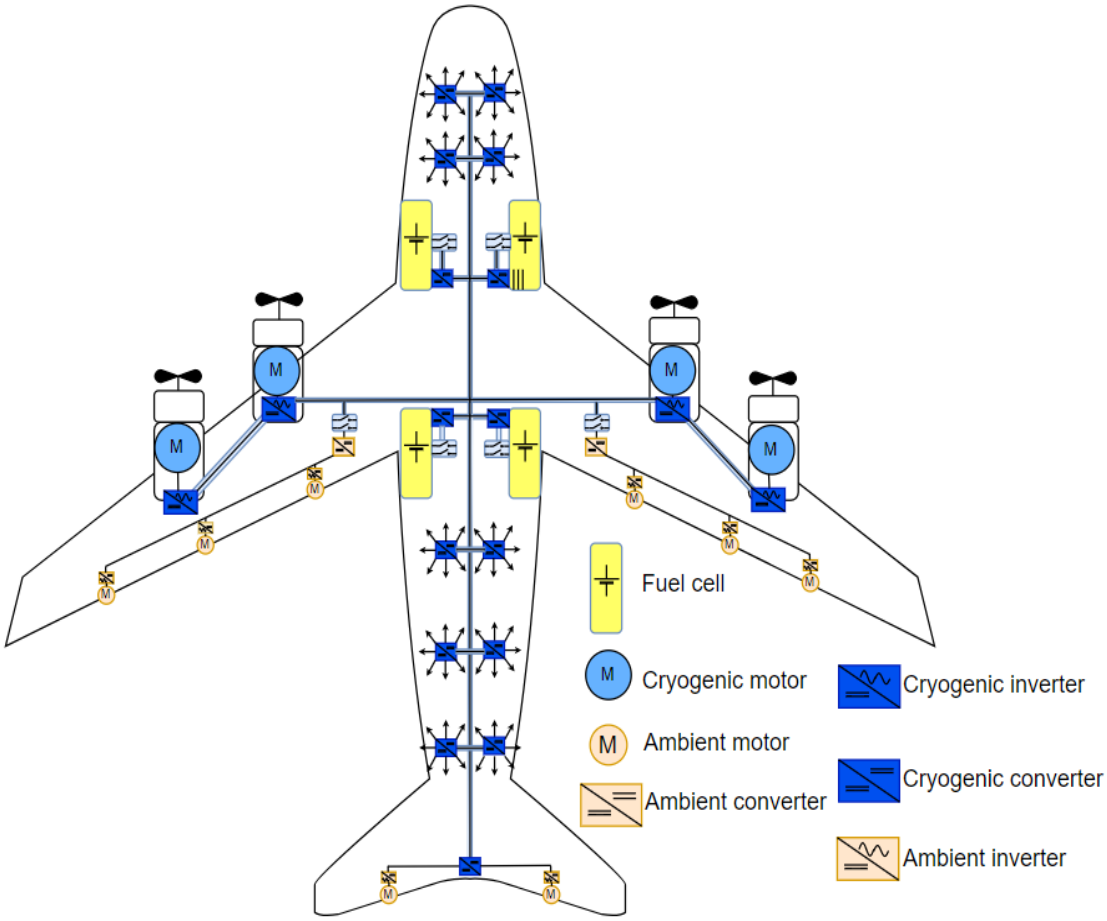

FIGURE 2. Architecture of hydrogen propulsion all-electric aircraf.

the best operating voltage taking into account the limits imposed by Paschen's law.

Figure 2 shows a simplified layout of an electric aircraft that is based on the design introduced in [11], where fuel cells would be used as the main power source for the prime mover. The fuel cells would be connected to a cryogenic DC/DC converter to step and regulate their voltage. The power would be transmitted over superconducting cables that are cooled down to cryogenic temperatures. These cables would supply, propeller motors, and auxiliary loads. From a thermal point of view, this architecture maintains a relatively similar temperature through the different components reducing the insulation weight thus making it mechanically less complex.

As seen from Figure 2 some of the components would operate at room temperature as the choice to switch over to cryogenic temperature would rely on how much power density is achieved. Large motors would benefit from utilizing superconducting technology to increase their power density. However, smaller motors used to steer the aircraft do not necessarily need to work at cryogenic temperature as they are small and the cooling insulation of the cooling could make them too heavy. Therefore, maintaining room temperature operation for these smaller motors is more feasible and efficient.

III. PERFORMANCE OF SEMICONDUCTOR DEVICES AT CRYOGENIC TEMPERATURES

Research has shown that power electronics devices' performance improves at lower temperatures and this is usually because the device's on-resistance ($R_{ds(on)}$), or the collector-emitter voltage (V_{CE}) in the case of IGBTs, decreases with temperature. The switching losses are also known to decrease as devices tend to switch faster with the decrease in temperature. This section reviews of the performance of different power electronic devices at cryogenic temperatures.

A. SI MOSFET

There have been significant studies on the performance of Si MOSFET at cryogenic temperature [8], [18], [19], [20], [21], [22], [23]. Table 1 shows the effect of cryogenic temperature on the device characteristics when the temperature of the device is between 50-100K. The on-resistance decreases at cryogenic temperatures. The breakdown voltage of the device is known to decrease with temperature. As for the switching losses, they tend to increase. Currently, for higher voltage applications, Superjunction MOSFETs are used as the device [13]. The highest voltage available device is 950V, this could be limited to be used in all-electric aircraft.

TABLE 1. Performance of semiconductor devices at lower temperatures.

Characteristic	Si MOSFET [18]-[23]	SiC MOSFET [24] – [27]	JFET [25], [28], [29]	IGBT [8], [30]-[33]	GaN [34] – [37]
On-resistance/ Forward voltage	Decreases 60%	Increases 70%	Increases by 3-120%	Decreases by 60%	Decreases by 80%
Breakdown voltage	Decreases 30-80%	Decreases 10%	N/A	Decreases by 30-60%	Increases by 10%
Switching losses	Decreases 90%	Decreases 10%	N/A	Decreases by 60-85%	Decreases by 25%
Gate source threshold voltage	Increases by 18-30%	Increases by 160%	N/A	Decreases by 18-90%	+15% and -25%

B. SiC MOSFET

SiC MOSFETs are attractive as they have lower switching losses and thermal capability than IGBTs at room temperatures. The literature presents studies on the performance of SiC devices at lower temperatures and found that the $R_{ds(on)}$ tends to increase by 70% at cryogenic temperatures. The breakdown voltage tends to decrease as well with the decrease in the temperature [8], [24], [25], [26], [27], [28]. The switching losses decrease by just 10% [27]. That significant increase in the SiC MOSFET RDS(on) makes the SiC MOSFET option unattractive.

C. SiC JFET

JFETs can have advantages over MOSFET in terms of reliability (robustness) and efficiency (lower resistance). References [25], [28], and [29] have tested several devices at cryogenic temperatures as shown in Table 1. From the table, it can be seen that the behavior of the devices is similar to that of the SiC MOSFET and this can be attributed that both devices are made of SiC, which tends to have worse characteristics at cryogenic temperatures. As shown the on-resistance of the devices can increase by 120%. Thus, they are not a preferred candidate for use at cryogenic temperatures.

D. IGBT

IGBTs are the most robust semiconductors that are currently available in the market at high power ratings. IGBT has shown a promising improvement at cryogenic temperatures [8], [30], [31], [32], [33]. The V_{CE} has been shown to decrease with the decrease in temperature. Switching losses have been shown to decrease with the decrease in temperature. The breakdown voltage decreases with the decrease in temperature. Thus, IGBTs are good candidates to be used at cryogenic temperatures. In [8], different types of IGBT modules were tested at low temperatures, where it was found that modules that contain Silicone gel tend to break down when immersed in cryogenic temperatures. Whereas devices that utilize epoxy resin, tend to withstand the harsh conditions of cryogenic temperatures.

E. GaN

GaN devices were reviewed in literature [34], [35], [36], [37], [38] where the devices were tested at cryogenic temperature and were found to significantly improve with the decrease in temperature [8]. The on-resistance decreased by almost 80% compared to its room temperature value. The switching losses showed a decrease of 25%. Based on this, GaN is the most compatible device to be used at lower temperatures. Currently, commercial GaN devices are not available at high power ratings, compared to those of SiC and IGBT modules, due to difficulty in manufacturing the dies [38]. GaN has also been shown to exhibit a phenomenon "Kink effect" at lower temperatures [39], where a rapid increase in the drain current provokes an increase in the conductance. The kink effect arises from the threshold voltage shift due to the forward biasing of the source-substrate diode caused by substrate impact ionization current flowing from the drain to the source. The magnitude of the kink effect is strongly dependent on the carbon concentration and the density of the background donors, thus for lower kink effect higher grade of substrate is needed. This needs further research to identify correct doping and substrate to lower kink effect at cryogenic temperatures.

F. SEMICONDUCTORS DEVICE'S POWER LOSSES

From the literature review completed in this section, it appears that there is limited information available on the JFET device's performance at cryogenic temperatures. Based on this, this article will mainly focus on the remaining four devices, Si MOSFET, SiC MOSFET, IGBT, and GaN. Figure 3 shows a comparison between the four devices, where it can be seen that SiC MOSFET performance degrades with the decrease in temperature, especially the RDS(on). Thus, SiC MOSFETs are not suitable candidates to be used for low temperatures. Si MOSFET, GaN, and IGBTs are more suitable for lower-temperature applications as can be seen from the figure.

G. AVAILABLE SEMICONDUCTOR DEVICE RATINGS

Currently, the highest ratings of available devices in the market is shown in Table 2. The highest voltage rating for Si MOSFET Infineon CoolMOS is 950V IPW95R060PFD7XKSA1. The highest rating available GaN is 1200V is the Transphorm (now Renesas) TP120H058WS (samples Q3 2024). As for the IGBT FZ1000R65KE4 6500V. Since the literature review done in Table 1 that most of the device's breakdown voltage decreases by about 30%, this would be difficult to implement circuits at higher voltage levels using commercial off-the-shelf (COTs) devices. Thus, a more complex circuit arrangement to adapt the semiconductor devices to perform at cryogenic temperatures.

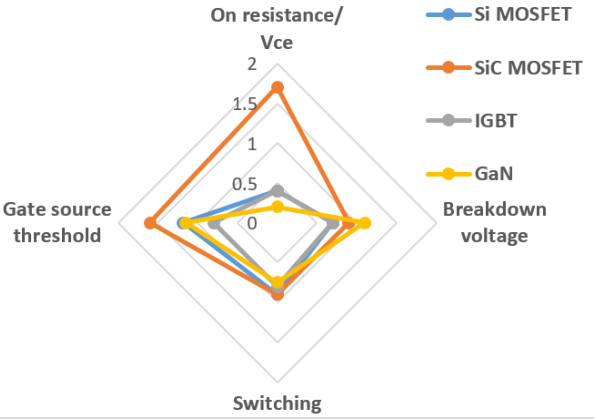

FIGURE 3. Losses of different semiconductor device.

References [40] and [41] tested devices in parallel at cryogenic temperature. In [40] an H-Bridge array of ten MOSFETs was connected in parallel and tested at cryogenic temperature. The experimental results showed that the devices were able to share the current equally because of the positive temperature coefficient.

TABLE 2. Commercial off the shelf device rating.

	Si MOSFET	GaN	IGBT
Manufacturer	Infineon	Transphorm	Mitsubishi
Voltage (V)	950	650	1700
Current (A)	74.7	95	600

IV. PERFORMANCE OF SEMICONDUCTOR DEVICES AT CRYOGENIC TEMPERATURES

Some passive components such as capacitors, and inductors immersed in liquid nitrogen tend to perform differently at cryogenic temperatures. In this section, this article reviews the performance of 1) capacitors, 2) inductors, and 3) resistors at cryogenic temperatures.

A. RESISTORS

Some certain types of resistors have shown resilience when immersed in cryogenic temperatures as their values did not change. In [42] different resistors were tested at room and cryogenic temperatures shown in Table 3. Wire wound and film resistors have shown a small change in value up to 5.7%. Whereas carbon and ceramic composition resistors experienced a significant change in their values and, therefore, they are not recommended for cryogenic temperature applications.

B. CAPACITORS

To optimize the performance of power electronics circuits at cryogenic temperatures, several types of capacitors were reviewed. Electrolytic capacitors, which are known for high energy densities, have shown that their capacitance almost reached zero due to the freezing of the electrolytes contained within them, thus making them unsuitable for cryogenic applications, as shown in Table 4. However, film and polypropylene capacitors have shown to be more resilient at much lower temperatures as their capacitance values experience modest alterations of up to 8%. Based on this review, film and polypropylene capacitors are suitable for applications at cryogenic temperatures. It must be noted, that even though these capacitors perform well at such low temperatures, they are physically bulky and would require larger space which is a challenging aspect in design for aircraft where space is an important restriction. Tantalum capacitors perform well at cryogenic temperatures with only a 10% decrease.

TABLE 3. Effect of cryogenic temperature on resistors.

Type	Change in Resistance (%) from 300K to 83K
Metal film	0.3
Wire wound	-0.6
Thick film	0.5
Carbon film	5.7
Carbon composition	28.0
Ceramic composition	17.6
Power film	4.1

C. MAGNETIC MATERIAL

Performance of magnetic materials were reviewed in [49], [50], and [51]. Figure 4 shows the performance characteristics of various magnetic materials across different temperatures, presenting their suitability for cryogenic applications. Ferrites experience a decrease in permeability as temperature decreases. Ferrites also experience a substantial increase in core losses at cryogenic temperatures, reaching up to 18 times compared to room temperature. On the other hand, nickel-iron alloys such as molyperm, permalloy, and mu-metal, as well as silicon steel, amorphous metals (metglas), and nanocrystalline materials (finemet and vitroperm) present a minimal permeability reduction of less than 20% at cryogenic temperatures, thus making them as superior candidates for such applications.

D. SUITABLE PASSIVE DEVICES

Based on this review, the selection of passive devices for cryogenic applications can be summarized as follows;

- Resistors; all types of resistors can be used at cryogenic temperatures except those of ceramic and carbon compositions.
- Capacitors; polypropylene, film, and tantalum capacitors are the best candidates for lower temperatures.
- Magnetic materials; ferrites have shown reduced permeability below 200K. Thus, it is not recommended to use

TABLE 4. Effect of cryogenic temperature on capacitors.

Capacitor Type	Capacitance at Cryogenic Temperature
Metalized polypropylene	Increased by 5% [43]
Polypropylene (Film/Foil)	Increased by 5% [43], [44], remained the same [45]
Polyethylene	Decreased by 5% [43], [44], [48]
NPO Ceramic	Slight increase by 1% [43], remained the same [45], [46]
Ceramic (X7R, Y5V)	Different results have been recorded for X7R as it decreased by 41% [43], and decreased by 80% [45], [48], Decreased at higher frequency [47], Y5V decreased by 50% [48]
Tantalum (TAJ)	Decreased 10% [44]
Tantalum (T491)	Decreased 10% [44]
Tantalum	Decreased 10% [44], [47], decrease by 20% [45]
Film	Decreased at 50 Hz by 8% [46]
Mica	Remained the same[44]
Polycarbonate	Slight decrease by 5%[45]
Polyphenylene	Remained the same [45], [48]
Z5U	Decreased up to 80% [45]
Al Electrolytic	Became zero [45]
Polyester	Decreased by 80% [48]

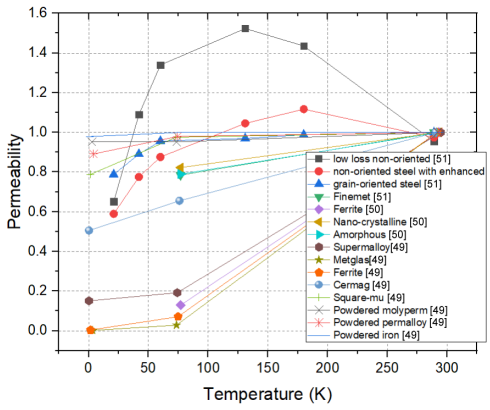

FIGURE 4. Performance of different magnetic material at lower temperatures.

them below that temperature. However, Nanocrystalline and Amorphouse

V. CIRCUIT TOPOLOGIES FOR CRYOGENIC POWER ELECTRONICS

This section will discuss the different circuit topologies for cryogenic power electronic circuits used in propulsion for all-electric aircraft. The section will review different topologies for both dc/dc converters and inverters to be used at

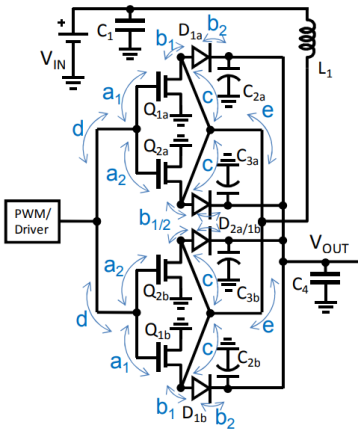

FIGURE 5. GaN quad devices for boost converter [55].

cryogenic temperatures. It will take into account the available COTS devices discussed in the previous section and the system voltage ratings discussed in Section II.

A. CONVERTER TOPOLOGIES FOR PROPULSION

Figure 2 has shown the electrical power distribution system, where it can be seen that a dc/dc converter is required to regulate the distribution voltage from the fuel cell, and that voltage is later stepped down to ±270 V for auxiliary supplies and 48 V for the avionics. In [9] a thorough review shows the different topologies of dc/dc converters that can be used at cryogenic temperatures. DC/DC converters can be divided into non-isolated and isolated converters. This section does a comparison with a recommendation in the end for the most appropriate option for all-electric aircraft.

1) NON-ISOLATED CONVERTERS

Non-isolated converters are converters that do not utilize transformers to step down or step up the voltage and do not necessarily require electrical isolation between the input and output sides. Non-isolated converters can be advantageous in the sense that they involve fewer components and hence higher efficiencies and are more cost-effective when compared to isolated converters. In [52], a ±270 V cascaded buck-boost converter has been proposed for the fuel cell for the aircraft. The converter was able to output power of 24 kW and had a power density of 8.3 kg/kW. In [53] has also done testing of two different configurations of buck-boost converters with a power rating of 15 kW, where a 2-level 4-switch buck-boost was able to achieve 44 kW/kg and a 3-level 8 switch was able to achieve 86 kW/kg. Interleaved non-isolated converters can be beneficial as they reduce the inductor size [54].

The articles [52], [53], and [54] mainly focus on power electronics circuits that are suitable for higher voltage using SiC MOSFETs that have high voltage ratings. This is mainly because COTS GaN devices are only available at lower voltage levels which was shown in Table 2. As a result, various research aims to address this limitation by using different inverter topologies to leverage GaN devices for high-power

applications. As an example, in [55], GaN devices were investigated by being put in parallel within a quad device setup for a non-isolate boost converter, where this configuration has achieved efficiency levels exceeding 99% for power outputs ranging from 600 to 3600W. Figure 5 shows a method for paralleling devices to increase the converter current rating. The four devices are interconnected to a common gate driver, effectively mitigating switching delays between devices and ensuring uniform current distribution.

Another example to overcome the rating of GaN device is that in [56] a multilevel boost converter, shown in Figure 6, can output voltages of 1 kV. That converter was able to reach a power density of 28.2 kW/kg and an efficiency of 99.3%.

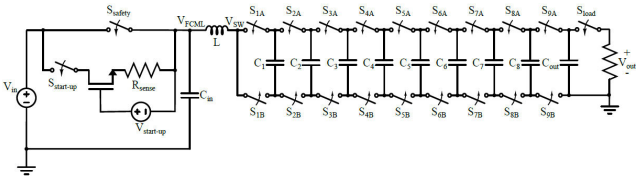

FIGURE 6. 10-level flying capacitor multilevel converter [56].

2) ISOLATED CONVERTERS

Isolated converters are converters that employ a magnetic transformer to isolate between the secondary and primary sides. Currently, most of the research on isolated converters has been focused on the two topologies of dual active bridge (DAB) and LLC converters as they are known to be robust and have high efficiency. The extended soft-switching on the primary and secondary side of the LLC converters makes them more efficient than DAB which can only do soft-switching on the primary, but their frequency control is more complex. In [57] a comparison has been made between Full-bridge (FB), half-bridge (HB) CLLC, and full-bridge and half-bridge DAB in terms of the cost, efficiency, complexity, and power density. The CLLC showed an overall higher efficiency over the DAB with the HBCLLC's highest efficiency of 96.5%.

For higher voltage levels, several articles have proposed a way around by using a multilevel configuration. In [58] a modular multilevel LLC has been proposed, which circuit diagram is shown in Figure 7. The authors were able to implement a converter for 3.6 kV with a rated power of 21 kW using a 6 Submodule configuration. A modulation strategy of quasi-square wave (QSW) was implemented and the converter was able to achieve an efficiency of 96.77%.

Another technique to design an LLC with a matrix transformer and split inductance is shown in Figure8 [59]. The authors were able to implement a 1 kV, 1 MHz converter by utilizing GaN devices. The efficiency of that converter was 95.18% with a power density of 107 W/inch3.

To select the proper topologies needed for commercial electric aircraft, several articles have reviewed the performance of different converters [52], [53], [54], [55], [56], [57], [58]. In [52], it was discussed an all SiC 2-level 4-switch buck-boost that was able to achieve 44 kW/kg with a 98.7%

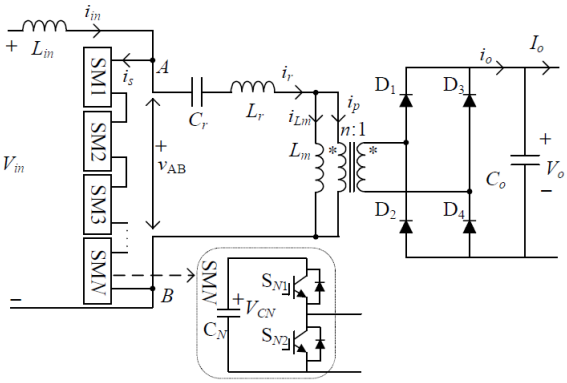

FIGURE 7. Modular Multilevel LLC resonant converter [58].

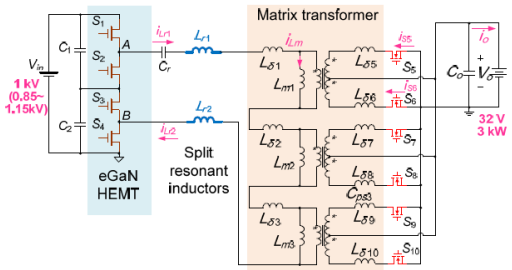

FIGURE 8. GaN LLC converter with matrix transformer and split resonant inductors [59].

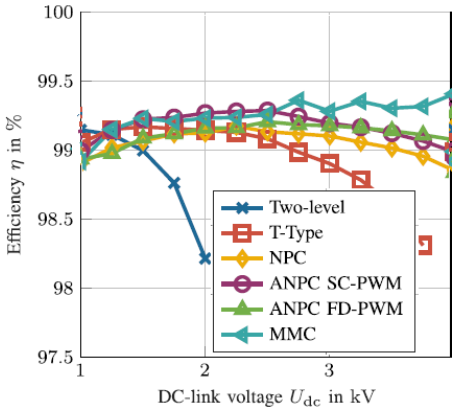

FIGURE 9. Comparison between the performance of the different inverter topologies efficiencies at different dc-link voltages, at (a) 10 kHz and (b) 30 kHz [62].

efficiency, and an all GaN 3-level 8-switch was able to achieve 86 kW/kg with a 98.2 % efficiency, however, the buck-boost converter lacks isolation and thus in case of a fault it would leave critical devices on the lower voltage end vulnerable. For higher voltage levels more modular designs of the converter have been proposed in [60] and [61].

B. INVERTER TOPOLOGIES FOR PROPULSION

Comprehensive analyses were carried out in [62], [63], and [64], where the articles examined various inverter topologies suitable for aircraft propulsion. The paper has examined the efficiency for different topologies including; 1) two-level, 2) T-type, 3) NPC, 4) ANPC, and 5) MMC. These different converter topologies. The number of semiconductor switches

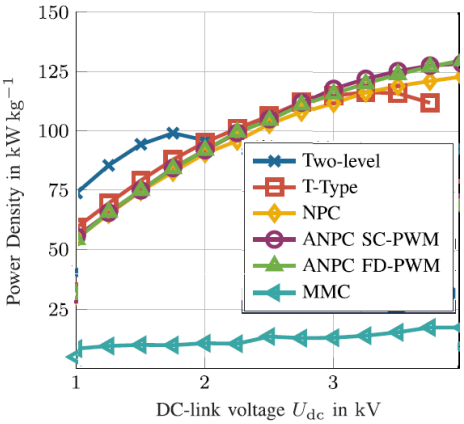

FIGURE 10. Comparison bet the performance of the different inverter topologies power densities at different dc-link voltages, at (a) 10 kHz and (b) 30 kHz [62].

can range from two switches per leg for the two-level inverter, a total of 6 switches for a three-phase inverter, up to six switches per leg for the ANPC, a total of 18 switches per a three-phase inverter, and the number of switches can be even higher for MMC type inverter. The higher number of switches means that more can be put in series and thus the inverter can withstand a higher voltage making it suitable to be used with GaN semiconductors that are only available at lower voltage ratings. As shown each topology requires a different number of semiconductor switches, this would affect the overall efficiency of the converter, and the power density is shown in Figure 9 and Figure 10 respectively.

As shown in Figure 9 where all converter operated at the same switching frequency of 30 kHz. From the figure, it can be seen that the two-level inverter has the highest efficiency at 1 kV, however, with the increase in the DC-link voltage the efficiency of the inverter sharply drops down to almost 98.25%. The main reason for that drop in efficiency is that the block and switching voltage is almost twice as high as that of a three-level inverter and even higher than the MMC. In the region between 2 to 3 kV NPC and ANPC seem to be the most reasonable choice as they still maintain a high efficiency and do not utilize a large number of components.

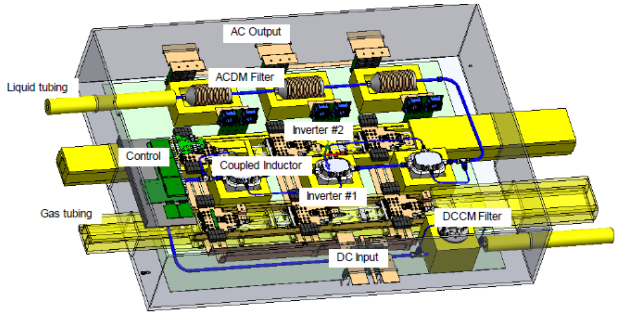

FIGURE 11. ANPC inverter integrated with cryogenic cooling [65].

Figure 10 shows the power density estimation of the different converter topologies at the same switching frequency of 30 kHz, from the figure it can be seen that the MMC inverter has a low overall power density compared to the other

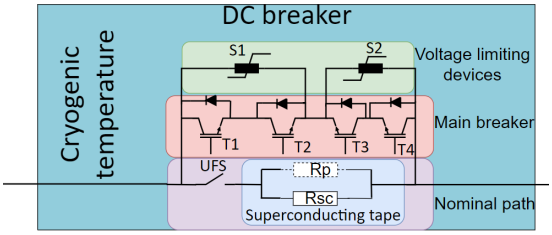

FIGURE 12. Hybrid DC-breaker with a SFCL.

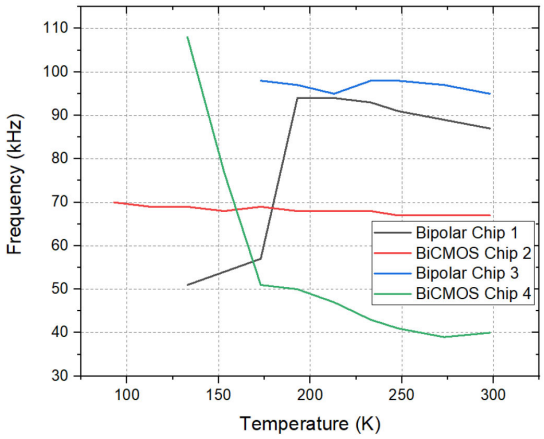

FIGURE 13. PWM ICs operating frequency vs temperature [70].

inverter topologies. For voltage levels between 1 kV to 2 kV two level inverters have the highest energy density. However, as the voltage level increases two inverters such as NPC, ANPC, and T-type have the highest power density. Based on these findings, we can eliminate the MMC inverter for not being suitable for aircraft mainly due to its very low power density. A two-level inverter will not be a viable solution if the network voltage is above 2 kV. This would leave the options down to NPC, ANPC, and T-type inverters. From the study done in [62], the T-type inverter seems to have a lower efficiency compared to the ANPC and the NPC. The T-type as well requires full DC voltage for the switches which limits it to less than 2 kV. This in the end would leave the choice between NPC and ANPC both of them have their advantage, as the NPC has a slightly higher power density than the ANPC due to the extra components, however the ANPC has higher efficiency because the lower conduction losses of the switches compared to diodes when clamping the neutral.

In [65] a cryogenically cooled ANPC inverter was tested where it was able to achieve a power density of 18 kVA/kg with a converter rated at 1 MVA shown in Figure11. The inverter utilized SiC MOSFET from CREE where it was cooled to 225K to avoid the breakdown of the module as it contains silicone gel in the structures. The inverter was able to achieve an efficiency of 99 %.

C. CIRCUIT BREAKER TOPOLOGIES FOR PROPULSION

Although motors on the aircraft use AC, transmission inside of the aircraft shall be done using DC via superconducting cables as seen in Figure2. In case of a fault, tripping on the AC

input side can be too slow as AC circuit breakers are known to be slow in the range of 3-5 cycles, for a 50 Hz, that would mean breaking the circuit in the of 60-100 milliseconds [65], which can cause the superconducting cable to heat till it fails. Thus, it was suggested to use solid-state DC breakers instead of electromechanical breakers as they are much faster to trip and would be able to protect the superconducting cable sufficiently. References [11], [66], and [67] review the different solid-state DC breaker topologies shown in Table 5. A superconducting fault current limiter hybrid breaker shown in Figure 12 offers protection due to the quenching effect of the superconducting for limiting the short circuit current.

TABLE 5. Different topologies of DC circuit breakers.

Configuration	Topology	Performance
Two branches	Passive resonance	Slower breaking time Easy configuration
	Current injection	Fast breaking time= 5ms Complex configuration
	Solid state	Fast breaking time= 5ms Very high voltage across the device during breaking
Three branches	Hybrid breaker	Fast breaking time= 5ms Lower voltage on semiconductor devices Lower voltage on semiconductor devices
	Current commutation hybrid breaker	Fast breaking time= 5ms Eliminates the need for semiconductors in the main path
	SFCL hybrid breaker	Fast breaking time= 5ms SFCL helps to limit the fault and eases the breaking of the circuit

The circuit breaker in Figure 12 mainly consists of three elements, 1) voltage clamping devices; used to protect the main breaker against over-voltages during a short circuit, 2) UFS and the superconducting tape; they are the main path during normal operation and when a fault occurs the superconducting quenches the fault so the current is directed into the third path and the UFS opens, 3) Main breaker; this consists of semiconductor switches that open during a short circuit event once the UFS is open. The choice of the semiconductor in the main breaker path does not have to be through low-losses devices at cryogenic temperatures as this is not the nominal path, and thus SiC MOSFET could be suitable to be used in that path. In case of a fault, the superconducting tape quenches, thus the current is diverted to the main switch through the semiconductor devices, and afterward, the UFS switch followed by the opening of the main breakers opens and the surge arrester clamps the voltage.

VI. PERFORMANCE OF LOGIC CIRCUIT AT CRYOGENIC TEMPERATURES

In [68] a study was done to understand the performance of different circuitries at cryogenic temperatures. The study investigated two CMOS 556 timer ICs, CMOS logic ICs, and two CMOS high-side driver ICs (IR2111), where all the tested devices seemed to have worked at cryogenic temperatures without a problem. Similarly, [69] has investigated the performance of the C2000 Texas Instruments DSP controller that utilizes the TMS320F28069 microcontroller in conjunction with the Texas instrument LM5113 gate driver both seemed to work fine at a temperature of reaching $-140°$. Using a microcontroller at a lower temperature would make the overall system less complicated and thus the research should focus more on this. In [70], an earlier generation microcontroller 8051 was tested at 70 K and was able to function well without a problem.

In [44], a total of four chips of two distinct PWM ICs using bipolar and CMOS technologies at cryogenic temperatures were tested and the results are shown in Figure13. It was shown that the chips that employed the bipolar technology tended to fail or stop working when their temperatures decreased down to 130K. Whereas, a single BiCMOS chip exhibited functionality even below 100K. These results were also substantiated by another study [19], where a bipolar technology was able to function 163K. It was determined that the bipolar technology ICs produced significant noise levels at cryogenic temperatures.

VII. PERFORMANCE OF GATE DRIVERS AT CRYOGENIC TEMPERATURES

To ensure that the power electronics circuits are working correctly, gate driver circuits must be close to the switching devices, which would mean immersing them at the same temperatures. For high power, the gate driver (no bootstrap diode) needs isolation between the controller and the semiconductor switch. Three types of gate driver isolations are mainly used; 1) magnetic isolation 2) capacitive isolation and 3) optical isolation. In this section, the gate drivers are reviewed.

A. POWER SUPPLY UNIT (PSU)

The main function of the power supply unit in the gate driver is to provide isolation between the primary and the secondary side. In [72], [73], [74], [76], and [77], different gate driver circuit topologies were tested at cryogenic temperatures. The power supply units tested in [72] are shown in Table 6, where some of them either reduced efficiency, resulted in failure, or inconsistency that has to do with the increased losses in ferrites Section IV.

B. SIGNAL TRANSMISSION

There are different types of signal transmission, either capacitive, inductive, or optical. References [72], [73], [74], and [75] tested the performance of the capacitive isolated gate drivers at cryogenic temperatures, whereas in [72] three different chips were tested and two of them seemed to stop working after reaching a temperature of 93 K and one chip (SI8271-GBD-IS) was able to perform well up to 77 K.

References [76] and [77] have used magnetic isolation for signal transmission. In [76], a COTS ferrite core was

TABLE 6. Commercial off the shelf psu rating.

Configuration	Topology	Watts	Performance
PEM2-S5-D5-S	CUI INC	2	-30%
PEME1-S12-S12-S		1	-34%
MDS01M-12	Meanwell Web	1	-24%
MDS01L-12		1	Failure
TRV 1-1212M	Traco Power	2	Failure
RV-0509S	Recom Power	2	Negligible
R05P209S		2	Negligible

used at cryogenic temperature. Even though the core had increased losses at that low temperature, the signal transmission remained correct. In [77], a nanocrystalline core was selected for the signal transmission and the power supply unit. The magnetic core has been shown to withstand lower temperatures. The structure for that gate driver is shown in figure 14.

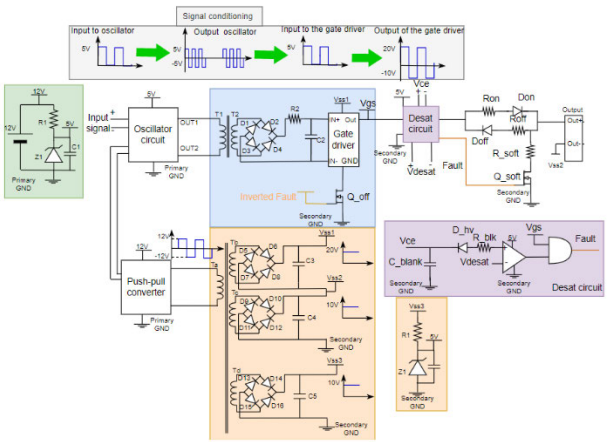

FIGURE 14. Cryogenic gate driver [77].

As for utilizing optocouplers for lower temperatures, the authors have tested some different IC HCPL-050L-000E which was found to stop working at cryogenic temperatures.

The review for cryogenic gate drivers can be summarized as shown in Table 7. Where using Nanocrystalline for cryogenic gate drivers is the most advantageous option as there is no loss in efficiency.

TABLE 7. Performance of different drivers at cryogenic temperature.

Configuration	Topology	Watts	Performance
COTS [72]	PSU	Ferrite	Reduction in efficiency or fails
	Signal transmission	Capacitive coupling	One out of three chips operational
		Ferrite	Operational
Lab built [77]	PSU	Nanocrystal line	Operational
	Signal transmission	Nanocrystal line	Operational

VIII. SENSING CIRCUITS AT CRYOGENIC TEMPERATURES

A. CURRENT SENSING

As current sensing [78] is critical for different aspects of control and protection, a robust current sensor is required to operate at the extreme conditions of cryogenic temperatures. There are different current sensing techniques reviewed in [78]. These include; 1) shunt resistor, 2) current transformers, 3) Rogowski coils, and 4) Hall-effect sensors. Although the shunt resistor measuring technique is the most straightforward to implement, however, it does not offer inherent galvanic isolation and can result in large conducting losses as well of the inductive component of the resistor. Current transformers and Rogowski coils provide low losses and galvanic isolation but are restricted to use with AC current waveforms.

Hall Effect current sensors can provide galvanic isolation and accurate measurements. However, there is scarce research on Hall Effect sensors for current at cryogenic temperature. COTS Hall effect current sensors require processing circuits to convert the signal, these circuits typically have bipolar junction transistors that do not perform well at cryogenic temperatures. However, some manufacturers such as Lakeshore [79] have developed Hall Effect sensors to be used to measure general magnetic field but did not accustom that for current sensors at cryogenic conditions. For cryogenic specific applications, CERN has developed a current transform DCCT [80], [81], [82] based on fluxgate current sensing. The key elements of a DCCT are 1) three magnetic cores carrying an arrangement of compensating win con dings, 2) an amplifier, 3) magnetic field detection circuitry, and 4) a sense resistance [81]. Figure 15 shows the figuration of a DCCT suggested in which a zero-flux compensation technique has been used for both AC and DC currents to achieve the current transformer ratio of $N_1I_1 = N_2I_2$. The cores of the CryoDCCT are wound with a tape of soft Ni 81-Mo 5-Fe magnetic alloy (referred to as cryogenic permalloy [83]), however there is a scarcity of information on how does this alloy compare with other magnetic materials at cryogenic temperatures.

B. VOLTAGE SENSING

Similar to current sensing, voltage sensing is important for both control and protection. There techniques of sensing the voltage are similar to that of current sensing and can include; 1) direct measurement or voltage divider, 2) voltage transformer, or 3) voltage amplifier, 4) Hall-effect sensor. The issues that arise from current sensing does not necessarily appear again in voltage sensing especially as the sensing wires can be extended and measured outside the cryogenic medium in ambient temperature with the processing circuit outside the extreme environment.

TABLE 8. Available commercial devices.

Technology	Manufacturer	Part number	Cost	Voltage (V)	Current (A)	Rds(on)/VCE (300K)	Rds(on)/VCE (77K) (Expected)
Si MOSFET	Infineon	IPA95R450P7	$	950	14	450 $m\Omega$	180 $m\Omega$
		IPA70R360P7S	$	700	12.5	360 $m\Omega$	144 $m\Omega$
SiC MOSFET	OnSemi	NVHL020N090SC1	$	900	118	20 $m\Omega$	34 $m\Omega$
	Infineon	IMDQ75R008M1H	$	750	173	7.8 $m\Omega$	13.3 $m\Omega$
	Microchip	MSCSM170AM029CT6LIAG	$$$$$	1700	676	2.9 $m\Omega$	4.93 $m\Omega$
		MSCSM120AM02CT6LIAG	$$$$$	1200	947	2.1 $m\Omega$	3.57 $m\Omega$
Si IGBT	Mitsubishi	CM600DX-34T	$$$	1700	600	2.1V	0.84 V
		CM800DX-24T1	$$$	1200	800	1.9V	0.76 V
GaN	VisiC	VM022HB065ST1AB11X00	Not available	650	460	2.2 $m\Omega$	0.44 $m\Omega$
		VM800HB65-S2AB1	Not available	650	800	8 $m\Omega$	1.6 $m\Omega$
Gate source threshold voltage	GaN Systems	GS-065-060-5-B-A	$	650	60	25 $m\Omega$	5 $m\Omega$

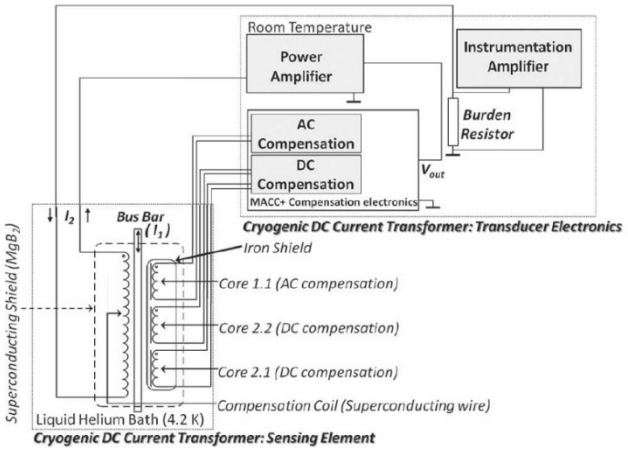

FIGURE 15. DCCT connection and operation [81].

IX. ELECTRICAL DISTRIBUTION SYSTEM AND CONVERTER TOPOLOGIES

Based on the literature done in the previous sections, this section mainly focuses on selecting the components and circuit topologies that would be suitable for the All-Electric Aircraft presented in Figure 2. In this section, the topologies and the final circuitry of the aircraft will be discussed. The section will do a market survey with the current semiconductor device technologies that are available and a selection of topologies and circuits based on this research. Figure 16 shows the distribution inside the all-electric aircraft which mainly consists of three parts; 1) network for actuator motors, 2) network for the main motors, and 3) network for the auxiliary loads. Each of them will be discussed in this section with the recommended topologies and semiconductor switches. This section will also give a list of COTS semiconductors that can be used at cryogenic temperatures.

A. MAIN DISTRIBUTION VOLTAGE

The main distribution network shown in Figure 16 shown in cyan would be used to feed all the power to the loads. The electrical distribution network has been previously discussed in [9] and [84], where the voltage level of the distribution network has been discussed to be either 3 kV for aircraft models proposed by Airbus or 540 V for the NASA 57-X aircraft. However, since superconducting cables would be used in LN2 conditions, the partial discharge would be around 7.6 kV/mm [85], making the 3 kV distribution network unfeasible to use. A voltage level of 3 kV is not present in the MIL-STD-704 and DO-160 standards. The main power circuits of that network as shown in Figure 16 would be 1) hybrid circuit breakers, 2) cryogenic inverter, and 3) cryogenic converters. The voltage of the distribution would affect the choice of the topology.

B. ACTUATOR MOTORS

EMA or EHA are the two primary types of actuator motors. It is preferable to employ the EHA function on principal control surfaces like elevators, ailerons, and rudders. The main factors affecting efficiency and comfort are secondary control surfaces like slats and flaps. While jamming is a possibility, operation via EMA is feasible. The Boeing 787's brakes can also be engaged via EMA [9]. It is anticipated that the voltage level of the actuator motors in Figure 16 will be 540V or ±270V [85], [86]. It is anticipated that these actuators will produce 100 kW of power [9], and at this power level, conventional power electronics are the most feasible option.

C. AUXILIARY LOADS

There are different types of auxiliary loads in the aircraft, such as ECS compressors, recirculation fans, galley fans, window heaters, avionics, and cargo heaters [87]. All of these loads have different voltage requirements ranging between 270V down to 28V. The power at his level can be in the range of 250 kVA. Room temperature inverters and converters can be used for these loads as they do not require as much power as the previous loads.

D. AVAILABLE COTS SEMICONDUCTOR DEVICES

The voltage ratings available for semiconductors are the main determinant of the topologies to be chosen. Table 8

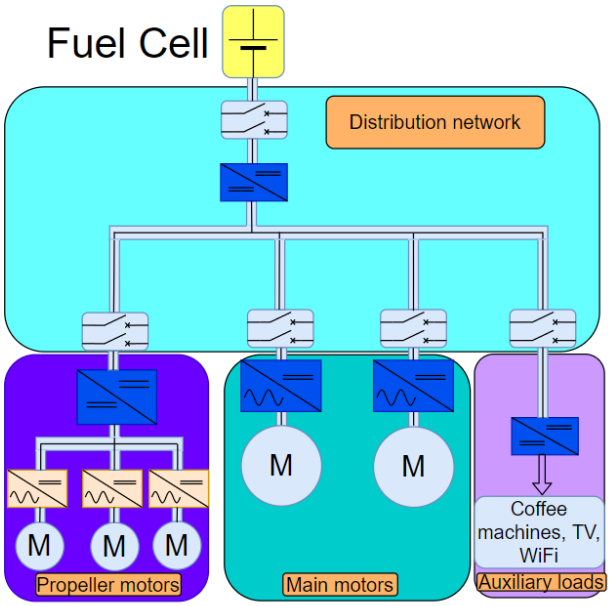

FIGURE 16. Electrical distribution network on All-Electric Aircraf.

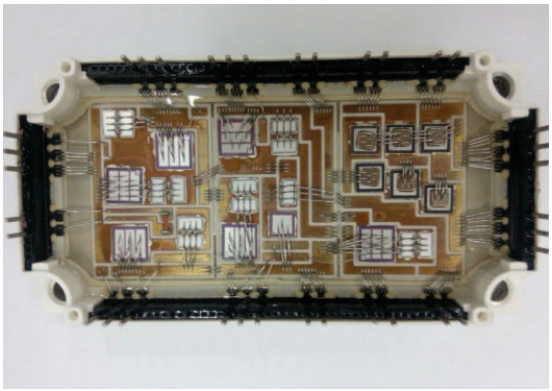

FIGURE 17. Generic power module with bond wire structur.

shows the list of different devices suitable for cryogenic temperatures their voltage ratings and the technology they utilize. Si MOSFET although their characteristics improve at cryogenic temperatures, their Rds(on) decreases with temperature their value is still higher than comparable technology. On the other hand, GaN devices Rds(on) is expected to be as low as 0.44 $m\Omega$ for a 460A for the device VM022HB065ST1AB11X00, however, their voltage range is much lower than SiC MOSFET and Si IGBT and would require more complex topologies changing the power density of the inverter/converter as it would drop. Therefore, for higher voltage levels, SiC MOSFET and Si IGBTs are preferable. In terms of conduction losses, SiC MOSFET is expected to have lower conduction power losses than Si IGBTs at room temperatures, however, with the significant reduction in the collector-emitter voltage at cryogenic temperatures, Si IGBTs are the more reliable candidates to be used. Based on this analysis, the following can be concluded:

- For 3 kV; Si IGBT should be used as they have higher efficiency at cryogenic temperature and would increase the overall system power density. The ratings of the IGBT shown in Table 8 mean that a multilevel topology is needed for the 3 kV. As per the discussion in the previous section, ANPC and NPC are the best contenders. As for the DC/DC conversion, that is done through an isolated ANPC or a multilevel converter as it achieves synchronous rectification which can not be done in the NPC topology.
- For 540 V; GaN modules should be used as their losses go steeply at 77 K. Based on the voltage level in Table 8 a 3L-ANPC is recommended as well.
- For 270 V and less; if these are to be operated at room temperatures, then SiC MOSFET or GaN DEVICES are the most suitable devices as they have the lowest losses at that temperature. All of the SiC MOSFET and GaN devices in Table 8 can accommodate the 270 V requirements, thus no need for a special multilevel inverter arrangement.
- In [8], the traditional module structure shown in Figure 17 has tended to always fail at cryogenic temperatures. However, the solid cover (SLC) shown in Figure 18 modules did not fail at cryogenic temperatures due to them having different structures and using epoxy resin as their insulation gel that can withstand more extreme temperatures. To objectively determine the reliability of a device and determine the failure of wire bonds failure, it is known through literature that two main tests can be done; 1) thermal cycling and 2) power cycling [88], [89], [90], [91], [92]
- To replicate the thermal stress of the operating environment, power modules that have undergone thermal cycling are repeatedly subjected to temperature changes within a cryogenic range or the operating range of the power electronics circuit. Because it replicates real-world settings where devices experience frequent temperature changes, this procedure is essential for evaluating the dependability and lifetime of power modules. Solder junctions, bonding wires, and encapsulating materials are especially susceptible to mechanical stress and strain during heat cycling because of the differential expansion and contraction of materials [88], [89]. This may lead to deterioration processes like delamination,

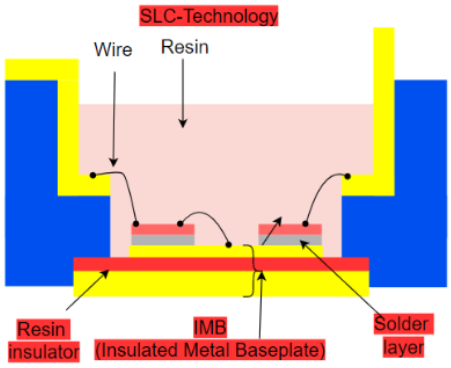

FIGURE 18. Solid cover architecture module [8].

the development of cracks, and ultimately the module's failure.

X. CHALLENGES OF CRYOGENIC POWER ELECTRONICS

This section mainly addresses the challenges facing cryogenic power electronics for all-electric aircraft. To assist tackle these problems, further research is needed.

A. RELIABILITY

Currently, all of the available COTS components are engineered to have the best possible characteristics for temperatures between −55° and 150°. By subjecting the COTS to extremely cold conditions, the mechanical integrity of the device becomes at risk. The main issue that causes the failure of the part is the different values of the coefficient of thermal expansion. Leading to the lift-off of the bond wires. Figure 18 shows, where the bond wires are used to connect the gate, drain, and source externally. The lifespan of the power modules is directly correlated with the dependability of the bonding wires; if the wires malfunction, the modules will experience electrical failure.

Currently, there is a very small of amount literature on testing the reliability of the devices through thermal and power cycling. In [93], SiGe voltage-controlled oscillators were investigated by subjecting the device to only 12 cycles between −195° and +85° at a temperature rate of 10°/min. It was found that the device performance has not changed. In [94], only 10 power cycles were done for a discrete MOSFET module IRF630. Although the MOSFET has shown no deviation from its characteristics, the number of cycles is too small to confirm the reliability of the device.

To ensure reliable performance of devices at cryogenic temperatures, testing should adhere to standards such as MIL-STD-883 or JEDEC JESD22-A104, with modifications to accommodate cryogenic conditions. Following these tests, the mechanical and electrical characteristics of the device must be evaluated to verify that it continues to function as intended.

B. COOLING PENALTY

To evaluate the advantages of placing electronics inside the cryostat, it is essential to understand the efficiency of the cooling process. If placing an element inside the cryostat results in a greater reduction of losses than the cost of cooling it, it is deemed beneficial. The cooling process efficiency is constrained by both the Carnot cycle efficiency and the efficiency of the cooler itself. The COP can be expressed as follows: $Q/P = \eta \cdot \eta_c$. where Q is the heat lifted from the cooler, P is the power used by the cooler, η the efficiency of the cooler, η_C the efficiency of the Carnot cycle, which is defined by $\eta_c = 1\text{-}T_c/T_h$, this would depend on the ambient temperature that surrounds the cryocooler and the target temperature required to operate the power electronics devices. Based on the review done in [95] and [96] the efficiency of the cryocooler would be a max of 0.2. For the all-electric aircraft, the ambient temperature surrounding the cryocooler can be either 300 K, or it can be engineered to inlet cold during the flight and have an ambient temperature of 215 K. The efficiency of the cryocooler would significantly increase as shown in Table 9. In [93] a synchronous buck converter efficiency was tested at room and cryogenic temperatures, where the efficiency came out to be 98% and 99% respectively for a 100 W converter, with a 1 W loss difference. To remove that 1 W, based on Table 9, 10 W is needed. Thus, in total cryogenic power electronics have more losses.

TABLE 9. Cooling penalty calculation.

	T_C	T_h	COP
Insulated	77	300	6.9%
Non-insulated	77	215	11.1%

However, there is an argument in the scientific community that since the low-temperature hydrogen on the aircraft will not be discarded after cooling the superconducting machine, it can be utilized for cryogenic power electronics. Thus, the cooling penalty should not apply to cryogenic power electronics because the hydrogen would be reheated and the efficiency should be evaluated in absolute terms [97]. Figure 19 shows suggest cooling system of the aircraft by the authors, where a cryotank would be used to supply the superconducting machine with hydrogen to maintain cold temperatures and then the output of that would be supplied to the power electronics circuits that would operate a temperature relatively high than that of the motor. Finally, the hydrogen would supplied to the fuel cell. As shown in the figure pressure regulators shall be used to control the pressure of the LH2 and flow. In order to implement such system feedback control is essential. The control would be monitoring the following;

1- Temperature sensor: making sure that the temperature in each region stays within the required values.
2- Pressure control: To make sure that the pressure within the system is maintained and there is no leakages.
3- Flow sensor: to control the flow of the hydrogen to maintain the required system temperature and pressure.

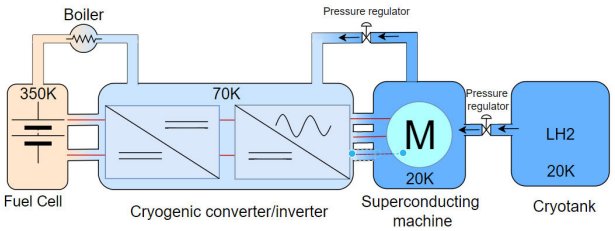

FIGURE 19. Suggested cooling system for the aircraf.

To ensure the reliability of cryogenic system, redundancy and fail-safe mechanism should be implemented. This can include an installation of a secondary backup cryotank, pressure regulators, pressure relief valves, and emergency shutdown. Further analysis of the cooling system needs to be

done, however, as this article is a top level review it is beyond its scope.

C. CRYOGENIC CONVERTER INSULATION WEIGHT

The weight of the cryostat, which is essential for maintaining cryogenic temperatures, is affected by different factors which include; the materials used for the cryostat, the type and the thickness of the insulation, the support structure for the cryostat, and the piping to and from the container. The size and the power losses of the power electronic circuit immersed in the cryogenic temperature play an important role. All of the attributes make it complex to determine the exact weight and overall complexity of the system. However, the following should be studied when building up a system;

1) MATERIALS USED FOR THE CRYOSTAT

The commonly used enclosing materials of the cryostat are either steel 304/304L dual grade or aluminum [98], [99]. This is a choice that has to a balance between durability, cost, and weight. To reduce the weight of the system as much as possible to maintain high power density, an aluminum structure is required.

2) INSULATION TYPE AND THICKNESS

Although foam insulation has an apparent mean thermal conductivity of 26-50 mW/mK between 77 K and 300 K, it is very inexpensive and still employed. However, this figure is significantly higher than that of a vacuum jacketed piping with MLI, which can reach a mean insulation level of 0.03-1 mW/mK, this range is affected by the vacuum quality with the upper end more typical of a flexible line field installation and the lower end more typical of a well-controlled laboratory environment [100], [101].

3) CONVERTER/INVERTER SIZE

The size of the power electronic circuit housed in the cryostat can affect the weight and power required by the cryostat when the volume of those circuits and the power losses are high. Therefore, efficient design strategies, control, and compact design must be employed with the design of these circuits.

D. SAFETY AND CERTIFICATION

In [9], the certification and safety of hydrogen-powered aircraft are critically reviewed, highlighting the contentious nature of hydrogen-related technologies in aviation. Hydrogen is a highly flammable substance as it has a flammability limit of 4% compared to that of kerosene with a 1.4% limit. Even though hydrogen's ignition temperature is higher than that of Kerosene's at 550° to 220°. Its minimum ignition energy is dramatically lower at 0.02 mJ as opposed to that of Kerosene's at 0.25 mJ. Meaning that hydrogen is much more likely to ignite with a very weak spark.

In addition to being flammable, hydrogen is odorless as well, making the management of leaks challenging. The development of a novel gas leakage detection system, fire detection devices, and prevention techniques are essential to ensure the safety of electric aircraft. The storage of hydrogen at cryogenic temperature also introduces additional hazards, for example, large spillages can rapidly condense the surrounding air, forming cold clouds that can drift over large areas [102]. Despite these challenges current research which has done models and experiments, suggests that hydrogen can be as safe as Kerosene for aviation use, provided that there are robust systems in place.

In [103] has highlighted on the methods and mitigation of leakage hydrogen, for example sensors can be installed close to the components that utilize hydrogen; these sensors can have detectors that can measure the concentration of the hydrogen or the temperature inside an enclosed space. It is recommended that threshold be set at 1% volume in air which 25% of the hydrogen lower flammability limit. Other assistive elements such as sprinklers, water curtains, inert gas such as nitrogen and ventilation can be used for further protection.

Recently hydrogen has made significant progress in the certification process as the FAA issued a G-1 paper in [104]. Where currently there are tests conducted to meet the airworthiness and safety requirements.

XI. CONCLUSION

The transition to sustainable all electric aviation demands a solution that is able to meet high power density and high efficiency. Thus article investigates the design consideration for the all-electric aircraft by particularly examining cryogenic propulsion where the transformative impact that hydrogen is expected to have on the aviation sector. In addition to being a clean energy source for the aerospace industry, hydrogen plays a critical role in enabling high-power density technologies like cryogenic power electronics and superconductivity. These innovations offer a more realistic perspective on the goal of all-electric aircraft. This article is mainly focused on cryogenic power electronics, how it is a key enabler in cryogenic propulsion as semiconductor have lower losses, faster switching and thus high power density at cryogenic temperature. These advancements are particularly significant in the context of cryogenic propulsion systems, where the synergy between cryogenic environments and power electronics paves the way for all-electric aircraft.

Nevertheless, using such technologies at such low temperatures presents difficulties, particularly with cryogenic power electronics. This publication's primary goal is to examine the potential electrical power systems for all-electric commercial airplanes. The conventional AC distribution system needs to be replaced with a DC system with a higher voltage level due to the increasing energy demand. Critical electrical components such as power converters and circuit breakers must achieve maximum power density to make aircraft electrification an attainable target.

The article has made a review of the performance of various semiconductor devices at cryogenic temperatures mainly to understand their suitability to be used at those extreme conditions. It was demonstrated through the literature review

that devices with lower conduction and switching losses, such as Si MOSFETs, IGBTs, and GaN technologies, are better suited for such low temperatures. Utilizing cutting-edge technology like GaN allows for the development of circuits with substantially greater power densities since these circuits' losses decrease most sharply when conduction losses approach 80% of their room temperature value.

The choice of passive elements would affect the performance of the circuit greatly. As discussed in the review of the previous sections; electrolytic capacitors tend to not function at all at cryogenic temperatures. Polypropylene and film capacitors are the best options. When it comes to magnetic material, ferrites are not suitable for such low temperatures, and would be recommended to use a nanocrystalline or an amorphous core. As for resistors, except for ceramic type, they are not generally affected by cryogenic temperature. Accordingly, the power electronics circuit would function properly provided the designer carefully selected the passive components at cryogenic temperatures.

For power electronics circuits, the article has gone through converter and inverter topologies have been briefly discussed in the article to accommodate power electronics circuits at cryogenic temperatures. It was shown that by using multilevel topologies the efficiency of the converter increases and has higher power density. These topologies are facilitators of using cryogenic devices at lower temperatures as semiconductor devices are known to have lower breakdown voltage at cryogenic temperatures and by putting them in series, this would increase the likelihood of them surviving a fault that is induced at cold temperatures. In addition to converters and inverters, the article has discussed the suitable dc-circuit breakers to be used at cryogenic temperatures, where hybrid circuit breakers that utilize SiC MOSFET and superconducting tape can be rapidly quenched and disconnect a fault. Another aspect of the power electronics circuit that the article covered is the cryogenic gate driver. Where it was shown that optic and capacitive gate drivers do not survive well at cryogenic temperatures and that using magnetic isolation is the best solution so far to have a robust circuit.

While semiconductor modules like SiC MOSFET are commonly used for room temperature circuits, Si IGBT and GaN are superior options at lower temperatures, according to the review done on cryogenic power electronics, which also covered the anticipated final architecture layout of the all-electric airplane. Given the understanding that IGBT devices' breakdown voltage drops with temperature, a recommended circuit architecture has been given. Furthermore, the article has addressed the limitation of the low breakdown voltage of the available COTS devices by suggesting more tailored topologies.

Finally, the article has also discussed the challenges of cryogenic power electronics when it comes to reliability. As there are different temperature coefficients, some modules have tended to break down at cryogenic temperatures. There is scarce data on the thermal and power cycling of the devices at lower temperatures and thus the research should focus on testing the robustness of these components. There is as well a lack of literature on the required insulation for cryogenic power electronics circuits which can have a huge impact on the weight of the converter. In terms of using hydrogen as the source of fuel for electric aircraft, there is an increased risk of flammability, this in turn would make the certification of the aircraft more difficult.

REFERENCES

[1] Our World Data. *Global CO_2 Emissions Come From Aviation*. Accessed: Dec. 19, 2023. [Online]. Available: https://ourworldindata.org/co2-emissions-from-aviation

[2] *Zeroe*. Accessed: Dec. 23, 2023. [Online]. Available: https://www.airbus.com/en/innovation/zero-emission/hydrogen/zeroe

[3] *Rolls-Royce and EasyJet Set New World First*. Accessed: Dec. 23, 2023. [Online]. Available: https://www.rolls-royce.com/media/press-releases/2022/28-11-2022-rr-and-easyjet-set-new-aviation-world-first-with-successful-hydrogen-engine-run.aspx

[4] *University Researchers Moving Electrified Aviation Forward With NASA*. Accessed: Dec. 23, 2023. [Online]. Available: https://www.nasa.gov/aeronautics/university-researchers-moving-electrified-aviation-forward-with-nasa/

[5] A. Barzkar and M. Ghassemi, "Electric power systems in more and all electric aircraft: A review," *IEEE Access*, vol. 8, pp. 169314–169332, 2020.

[6] J. K. Nøland, "Hydrogen electric airplanes: A disruptive technological path to clean up the aviation sector," *IEEE Electrific. Mag.*, vol. 9, no. 1, pp. 92–102, Mar. 2021.

[7] S. Tiwari, M. J. Pekris, and J. J. Doherty, "A review of liquid hydrogen aircraft and propulsion technologies," *Int. J. Hydrogen Energy*, vol. 57, pp. 1174–1196, Feb. 2024, doi: 10.1016/j.ijhydene.2023.12.263.

[8] H. Gui, R. Chen, J. Niu, Z. Zhang, L. M. Tolbert, F. Wang, B. J. Blalock, D. Costinett, and B. B. Choi, "Review of power electronics components at cryogenic temperatures," *IEEE Trans. Power Electron.*, vol. 35, no. 5, pp. 5144–5156, May 2020.

[9] H. Schefer, L. Fauth, T. H. Kopp, R. Mallwitz, J. Friebe, and M. Kurrat, "Discussion on electric power supply systems for all electric aircraft," *IEEE Access*, vol. 8, pp. 84188–84216, 2020.

[10] A. Elwakeel, N. McNeill, R. P. Alzola, R. K. Surapaneni, G. Galla, L. Ybanez, M. Zhang, and W. Yuan, "Characterizing semiconductor devices for all-electric aircraft," *IEEE Access*, vol. 11, pp. 73490–73504, 2023.

[11] A. Elwakeel, E. Ertekin, M. Elshiekh, M. Iftikhar, W. Yuan, and M. Zhang, "Protection system architecture for all-electric aircraft," *IEEE Trans. Appl. Supercond.*, vol. 33, no. 5, Aug. 2023, Art. no. 5203707.

[12] A. Elwakeel, N. McNeill, R. Peña-Alzola, M. Zhang, and W. Yuan, "Cryogenic DC/DC converter for superconducting magnet application," *IEEE Trans. Appl. Supercond.*, vol. 32, no. 6, pp. 1–5, Sep. 2022.

[13] A. Elwakeel, Z. Feng, N. McNeill, R. P. Alzola, M. Zhang, and W. Yuan, "Comparison of phase-leg circuits for cryogenic operation in the all-electric aircraft," in *Proc. 11th Int. Conf. Power Electron., Mach. Drives (PEMD)*, Jun. 2022, pp. 618–624.

[14] F. Weng, M. Zhang, A. Elwakeel, T. Lan, N. McNeill, and W. Yuan, "Transient test and AC loss study of a cryogenic propulsion unit for all electric aircraft," *IEEE Access*, vol. 9, pp. 59628–59636, 2021.

[15] A. Elwakeel, Z. Feng, N. McNeill, M. Zhang, B. Williams, and W. Yuan, "Study of power devices for use in phase-leg at cryogenic temperature," *IEEE Trans. Appl. Supercond.*, vol. 31, no. 5, pp. 1–5, Aug. 2021.

[16] *Airbus.com*. Accessed: Feb. 8, 2024. [Online]. Available: https://www.airbus.com/en/innovation/low-carbon-aviation/hybrid-and-electric-flight/e-fan-x

[17] Y. Ji, P. Giangrande, W. Zhao, H. Wang, V. Madonna, H. Zhang, and M. Galea, "Moving towards partial discharge-free design of electrical machines for more electric aircraft applications," *IEEE Trans. Transport. Electrific.*, vol. 9, no. 3, pp. 4668–4679, Sep. 2023.

[18] Y. Chen, X.-Y. Chen, T. Li, Y.-J. Feng, Y. Liu, Q. Huang, M.-Y. Li, and L. Zeng, "Experimental investigations of state-of-the-art 650-V class power MOSFETs for cryogenic power conversion at 77K," *IEEE J. Electron Devices Soc.*, vol. 6, pp. 8–18, 2018.

[19] K. K. Leong, A. T. Bryant, and P. A. Mawby, "Power MOSFET operation at cryogenic temperatures: Comparison between HEXFET, MDMeshTM and CoolMOSTM," in *Proc. 22nd Int. Symp. Power Semiconductor Devices IC's (ISPSD)*, Jun. 2010, pp. 209–212.
[20] K. K. Leong, B. T. Donnellan, A. T. Bryant, and P. A. Mawby, "An investigation into the utilisation of power MOSFETs at cryogenic temperatures to achieve ultra-low power losses," in *Proc. IEEE Energy Convers. Congr. Expo.*, Sep. 2010, pp. 2214–2221.
[21] A. E. Schlogl, H. W. Lorenzen, U. Linnert, and J. P. Stengl, "Properties of CoolMOSTM between 420 K and 80 K-the ideal device for cryogenic applications," in *Proc. 11th Int. Symp. Power Semiconductor Devices ICs*, Aug. 1999, pp. 9–12.
[22] O. Mueller, "Switching losses of the cryogenic MOSFET and SIT," *Cryogenics*, vol. 30, no. 12, pp. 1094–1100, Dec. 1990.
[23] R. Singh and B. J. Baliga, "Power MOSFET analysis/optimization for cryogenic operation including the effect of degradation in breakdown voltage," in *Proc. Int. Symp. Power Semicond. Devices (ICs)*, Aug. 2005, pp. 339–344.
[24] H. Chen, P. M. Gammon, V. A. Shah, C. A. Fisher, C. W. Chan, S. Jahdi, D. P. Hamilton, M. R. Jennings, M. Myronov, D. R. Leadley, and P. A. Mawby, "Cryogenic characterization of commercial SiC power MOSFETs," *Mater. Sci. Forum*, vols. 821–823, pp. 777–780, Jun. 2015.
[25] T. Chailloux, C. Calvez, N. Thierry-Jebali, D. Planson, and D. Tournier, "SiC power devices operation from cryogenic to high temperature: Investigation of various 1.2kV SiC power devices," *Mater. Sci. Forum*, vols. 778–780, pp. 1122–1125, Feb. 2014.
[26] S. Chen, C. Cai, T. Wang, Q. Guo, and K. Sheng, "Cryogenic and high temperature performance of 4H-SiC power MOSFETs," in *Proc. 28th Annu. IEEE Appl. Power Electron. Conf. Expo. (APEC)*, Mar. 2013, pp. 207–210.
[27] H. Gui, R. Ren, Z. Zhang, R. Chen, J. Niu, F. Wang, L. M. Tolbert, B. J. Blalock, D. J. Costinett, and B. B. Choi, "Characterization of 1.2 kV SiC power MOSFETs at cryogenic temperatures," in *Proc. IEEE Energy Convers. Congr. Expo. (ECCE)*, Sep. 2018, pp. 7010–7015.
[28] R. L. Patterson, A. Hammoud, and M. E. Elbuluk. (Jul. 2005). *Switching Characteristics of JFET Transistors At Cryogenic Temperatures*. Accessed: Apr. 2, 2002. [Online]. Available: https://nepp.nasa.gov/files/11437/Switching%20Characteristics%20of%20JFET%20Transistors%20at%20Cryogenic%20Temperatures1.doc
[29] M. Iliescu and M. Culcer, "Experimental study about JFET's behaviour at low temperatures," *Romanian Rep. Phys.*, vol. 52, pp. 167–170, Jun. 2000.
[30] A. J. Forsyth, S. Y. Yang, P. A. Mawby, and P. Igic, "Measurement and modelling of power electronic devices at cryogenic temperatures," *IEE Proc. Circuits, Devices Syst.*, vol. 153, no. 5, p. 407, 2006.
[31] R. Singh and B. J. Baliga, "Cryogenic operation of asymmetric n-channel IGBTs," *Solid-State Electron.*, vol. 38, no. 3, pp. 561–566, Mar. 1995.
[32] K. Tian, J. Qi, Z. Mao, S. Yang, W. Song, M. Yang, and A. Zhang, "Characterization of 1.2 kV 4H-SiC power MOSFETs and Si IGBTs at cryogenic and high temperatures," in *Proc. 14th China Int. Forum Solid State Lighting, Int. Forum Wide Bandgap Semiconductors China*, Nov. 2017, pp. 140–143.
[33] Y. Wei, M. M. Hossain, and A. Mantooth, "Cryogenic static and dynamic characterizations of 650 v field stop trench Si IGBT," in *Proc. IEEE 22nd Workshop Control Modeling Power Electron. (COMPEL)*, Nov. 2021, pp. 1–6.
[34] J. Colmenares, T. Foulkes, C. Barth, T. Modeert, and R. C. N. Pilawa-Podgurski, "Experimental characterization of enhancement mode gallium-nitride power field-effect transistors at cryogenic temperatures," in *Proc. 4th IEEE Work. Wide Bandgap Power Devices Appl*, Nov. 2016, pp. 129–134.
[35] Z. Zhang, H. Gui, R. Ren, F. Wang, L. M. Tolbert, D. J. Costinett, and B. J. Blalock, "Characterization of wide bandgap semiconductor devices for cryogenically-cooled power electronics in aircraft applications," in *Proc. AIAA/IEEE Electr. Aircr. Technol. Symp. (EATS)*, Jul. 2018, pp. 1–8.
[36] R. E. Mayo, J. G. Bustamante, and T. Beechner, "Wide temperature range operation of GaN HEMTs for power dense energy conversion," in *Proc. 16th IEEE Intersociety Conf. Thermal Thermomechanical Phenomena Electron. Syst.*, May 2017, pp. 530–536.
[37] R. Ren, H. Gui, Z. Zhang, R. Chen, J. Niu, F. Wang, L. M. Tolbert, D. Costinett, B. J. Blalock, and B. B. Choi, "Characterization and failure analysis of 650-V enhancement-mode GaN HEMT for cryogenically cooled power electronics," *IEEE J. Emerg. Sel. Topics Power Electron.*, vol. 8, no. 1, pp. 66–76, Mar. 2020.
[38] A. Udabe, I. Baraia-Etxaburu, and D. G. Diez, "Gallium nitride power devices: A state of the art review," *IEEE Access*, vol. 11, pp. 48628–48650, 2023.
[39] I. M. Hafez, G. Ghibaudo, and F. Balestra, "Analysis of the kink effect in MOS transistors," *IEEE Trans. Electron Devices*, vol. 37, no. 3, pp. 818–821, Mar. 1990.
[40] W. Bailey, H. Wen, Y. Yang, A. Forsyth, and C. Jia, "A cryogenic DC–DC power converter for a 100kW synchronous HTS generator at liquid nitrogen temperatures," *Phys. Proc.*, vol. 36, pp. 1002–1007, Jan. 2012.
[41] T. Matsukawa, M. Shioyama, J. NOMURA, C. Neumeyer, S. Tsuji-Iio, and R. Shimada, "Synchronous rectifier using power-MOSFET for high current AC/DC converter system," in *Proc. Symp. Fusion Eng.*, Jun. 2003, pp. 80–83.
[42] A. Patterson and S. Gerber. (Aug. 2001). *Perfomance of Various Types of Resistors At Low Temperatures*. Accessed: Apr. 4, 2022. [Online]. Available: https://nepp.nasa.gov/DocUploads/47394B68-DE94-4525-95A6E2164342B9F4/LT-Test-Report-Resistors.pdf
[43] J. Garrett, R. Schupbach, A. B. Lostetter, and H. A. Mantooth, "Development of a DC motor drive for extreme cold environments," in *Proc. IEEE Aerosp. Conf.*, Mar. 2007, pp. 1–12.
[44] Bourne, R. Schupbach, B. Hollosi, J. Di, A. Lostetter, and H. A. Mantooth, "Ultra-wide temperature (−230 °C to 130 °C) dc-motor drive with SiGe asynchronous controller," in *Proc. IEEE Aerosp. Conf.*, May 2008, pp. 1–15.
[45] M.-J. Pan, "Performance of capacitors under DC bias at liquid nitrogen temperature," *Cryogenics*, vol. 45, no. 6, pp. 463–467, Jun. 2005.
[46] A. Hammoud and E. Overton, "Low temperature characterization of ceramic and film power capacitors," in *Proc. Conf. Electr. Insul. Dielectric Phenomena (CEIDP)*, vol. 2, Oct. 1996, pp. 701–704.
[47] A. Hammoud, S. Gerber, R. L. Patterson, and T. L. MacDonald, "Performance of surface-mount ceramic and solid tantalum capacitors for cryogenic applications," in *Proc. Annu. Rep. Conf. Electr. Insul. Dielectric Phenomena*, Atlanta, GA, USA, Aug. 1998, pp. 572–576.
[48] F. Teyssandier and D. Prêle, "Commercially available capacitors at cryogenic temperatures," in *Proc. 9th Int. Workshop Low Temp. Electron. (WOLTE)*, Guaruja, Brazil, Jun. 2010.
[49] M. Kokalj, B. Pinter, M. Lindic, B. Voljc, Z. Svetik, and R. Lapuh, "Realization of dissipation factor standard," in *Proc. CPEM*, Jun. 2010, pp. 426–427.
[50] S. Yin, M. Mehrabankhomartash, A. J. Cruz, L. Graber, M. Saeedifard, S. Evans, F. Kapaun, I. Revel, G. Steiner, L. Ybanez, and C. Park, "Characterization of inductor magnetic cores for cryogenic applications," in *Proc. IEEE Energy Convers. Congr. Expo. (ECCE)*, Oct. 2021, pp. 5327–5333.
[51] X. Pei, A. C. Smith, L. Vandenbossche, and J. Rens, "Magnetic characterization of soft magnetic cores at cryogenic temperatures," *IEEE Trans. Appl. Supercond.*, vol. 29, no. 5, pp. 1–6, Aug. 2019.
[52] M. Warncke, S. Fahlbusch, and K. F. Hoffmann, "DC/DC-converter for fuel cell integration in more electric aircraft applications," in *Proc. 19th Eur. Conf. Power Electron. Appl. (EPE ECCE Eur.)*, Warsaw, Poland, Sep. 2017, pp. P.1–P.10.
[53] D. Menzi, L. Imperiali, E. Bürgisser, M. Ulmer, J. Huber, and J. W. Kolar, "Ultralightweight high-efficiency buck-boost DC–DC converters for future eVTOL aircraft with hybrid power supply," *IEEE Trans. Transport. Electrific.*, vol. 10, no. 4, pp. 10297–10313, Dec. 2024.
[54] S. Gangavarapu and A. K. Rathore, "Analysis and design of interleaved DCM buck–boost derived three-phase PFC converter for MEA," *IEEE Trans. Transport. Electrific.*, vol. 7, no. 3, pp. 1954–1963, Sep. 2021.
[55] Y.-F. Wu, "Paralleling high-speed GaN power HEMTs for quadrupled power output," in *Proc. Twenty-Eighth Annu. IEEE Appl. Power Electron. Conf. Expo. (APEC)*, Long Beach, CA, USA, Mar. 2013, pp. 211–214.
[56] S. Coday, N. Ellis, Z. Liao, and R. C. N. Pilawa-Podgurski, "A lightweight multilevel power converter for electric aircraft drivetrain," in *Proc. IEEE Energy Convers. Congr. Expo. (ECCE)*, Vancouver, BC, Canada, Oct. 2021, pp. 1507–1513.
[57] P. He and A. Khaligh, "Comprehensive analyses and comparison of 1 kW isolated DC–DC converters for bidirectional EV charging systems," *IEEE Trans. Transport. Electrific.*, vol. 3, no. 1, pp. 147–156, Mar. 2017, doi: 10.1109/TTE.2016.2630927.
[58] Y. Chen, W. Chen, and C. Chen, "Modular multi-level LLC resonant converter for high-power and medium-voltage application," in *Proc. IEEE Int. Power Electron. Appl. Conf. Expo. (PEAC)*, Guangdong, China, Nov. 2022, pp. 16–20.

[59] K. Xu, Z. Zhang, Z.-W. Xu, M.-X. He, H. Li, X. Ren, and Q. Chen, "1-kV input 1-MHz GaN modular multilevel LLC converters," in *Proc. IEEE Appl. Power Electron. Conf. Expo. (APEC)*, Anaheim, CA, USA, Mar. 2019, pp. 2329–2336.

[60] N. Keshmiri, M. I. Hassan, R. Rodriguez, and A. Emadi, "Comparison of isolated bidirectional DC/DC converters using WBG devices for more electric aircraft," *IEEE Open J. Ind. Electron. Soc.*, vol. 2, pp. 184–198, 2021.

[61] X. Du, F. Diao, Z. Zhao, and Y. Zhao, "An all silicon carbide 3 kV/540 v series-resonant converter for electric aircraft systems," *IEEE Trans. Ind. Appl.*, vol. 58, no. 6, pp. 7363–7372, Nov. 2022, doi: 10.1109/TIA.2022.3191305.

[62] J. Ebersberger, M. Hagedorn, M. Lorenz, and A. Mertens, "Potentials and comparison of inverter topologies for future all-electric aircraft propulsion," *IEEE J. Emerg. Sel. Topics Power Electron.*, vol. 10, no. 5, pp. 5264–5279, Oct. 2022.

[63] M. Schweizer, T. Friedli, and J. W. Kolar, "Comparative evaluation of advanced three-phase three-level inverter/converter topologies against two-level systems," *IEEE Trans. Ind. Electron.*, vol. 60, no. 12, pp. 5515–5527, Dec. 2013.

[64] R. Yapa, A. J. Forsyth, and R. Todd, "Analysis of SiC technology in two1008 level and three-level converters for aerospace applications," in *Proc. 7th IET Int. Conf. Power Electron., Mach. Drives (PEMD)*, 2014, pp. 1–6.

[65] Y.-W. Jeong, H.-W. Lee, Y.-G. Kim, and S.-W. Lee, "High-speed AC circuit breaker and high-speed OCR," in *Proc. 22nd Int. Conf. Exhib. Electr. Distrib. (CIRED)*, Jun. 2013, pp. 1–4.

[66] M. Barnes, D. Vilchis-Rodriguez, X. Pei, R. Shuttleworth, O. Cwikowski, and A. C. Smith, "HVDC circuit Breakers–A review," *IEEE Access*, vol. 8, pp. 211829–211848, 2020.

[67] L. Chen, G. Li, H. Chen, X. Qiao, M. Ding, R. Hu, X. Deng, T. Ding, C. Hong, and J. Yang, "Combinatorial multi-objective optimization of resistive SFCL and DC circuit breaker in hybrid HVDC transmission system," *IEEE Trans. Appl. Supercond.*, vol. 31, no. 8, pp. 1–6, Nov. 2021.

[68] F. F. Perez-Guerrero, B. Ray, and R. L. Patterson, "Low temperature operation of a three-level buck DC–DC converter," in *Proc. 32nd Intersociety Energy Convers. Eng. Conf.*, vol. 2, Jul. 1997, pp. 1415–1420.

[69] C. B. Barth, T. Foulkes, O. Azofeifa, J. Colmenares, K. Coulson, N. Miljkovic, and R. C. N. Pilawa-Podgurski, "Design, operation, and loss characterization of a 1-kW GaN-based three-level converter at cryogenic temperatures," *IEEE Trans. Power Electron.*, vol. 35, no. 11, pp. 12040–12052, Nov. 2020, doi: 10.1109/TPEL.2020.2989310.

[70] M. E. Elbuluk, A. Hammoud, S. Gerber, R. Patterson, and E. Overton, "Performance of high-speed PWM control chips at cryogenic temperatures," *IEEE Trans. Ind. Appl.*, vol. 39, no. 2, pp. 443–450, Mar. 2003.

[71] M. Elbuluk, A. Hammoud, and R. Patterson, "Power electronic components, circuits and systems for deep space missions," in *Proc. IEEE 36th Conf. Power Electron. Spec.*, Mar. 2005, pp. 1156–1162.

[72] Mustafeez–ul–Hassan, Y. Wu, V. Solovyov, and F. Luo, "Liquid nitrogen immersed and noise tolerant gate driver for cryogenically cooled power electronics applications," in *Proc. IEEE Appl. Power Electron. Conf. Expo. (APEC)*, Mar. 2022, pp. 555–561.

[73] Mustafeez-ul-Hassan, Y. Wu, V. Solovyov, and F. Luo, "Investigation about operation and performance of gate drivers for power electronics converters for cryogenic temperatures," in *Proc. 24th Eur. Conf. Power Electron. Appl. (EPE ECCE Eur.)*, Hanover, Germany, Sep. 2022, pp. 1–9.

[74] Y. Wei, M. M. Hossain, R. Sweeting, and A. Mantooth, "Functionality and performance evaluation of gate drivers under cryogenic temperature," in *Proc. IEEE Aerosp. Conf.*, Mar. 2021, pp. 1–9.

[75] D. Qin, Z. Zhang, S. K. Dam, C.-H. Yang, Z. Dong, R. Chen, H. Bai, and F. Wang, "Intelligent gate drive for cryogenic solid-state circuit breaker with current limitation capability for aviation application," in *Proc. IEEE Appl. Power Electron. Conf. Expo. (APEC)*, Orlando, FL, USA, Mar. 2023, pp. 318–323, doi: 10.1109/APEC43580.2023.10131424.

[76] A. Deriszadeh, X. Zeng, R.-K. Surapaneni, G. Galla, E. Nilsson, J.-F. Rouquette, L. Ybanez, and X. Pei, "Gate driver design for cryogenically cooled power electronic converters," *IEEE Trans. Appl. Supercond.*, vol. 34, no. 3, pp. 1–6, May 2024.

[77] A. Elwakeel, N. McNeill, R. P. Alzola, R. K. Surapaneni, G. Galla, L. Ybanez, M. Zhang, and W. Yuan, "Design and testing of isolated gate driver for cryogenic environments," *IEEE Trans. Appl. Supercond.*, vol. 34, no. 3, pp. 1–4, May 2024.

[78] S. Ziegler, R. C. Woodward, H. H.-C. Iu, and L. J. Borle, "Current sensing techniques: A review," *IEEE Sensors J.*, vol. 9, no. 4, pp. 354–376, Apr. 2009.

[79] Default. *Hall (Magnetic) Sensors*. Accessed: May 30, 2024. [Online]. Available: https://www.lakeshore.com/products/categories/magnetic-products/hall-(magnetic)-sensors

[80] G. Montenero, P. Arpaia, A. Ballarino, and L. Bottura, "Design, assembly, and commissioning of a cryogenic DC current transformer designed for measuring currents of up to 80 kA," *IEEE Trans. Appl. Supercond.*, vol. 25, no. 3, pp. 1–6, Jun. 2015.

[81] G. Hudson and K. Bouwknegt, "4-13kA DC current transducers enabling accurate in-situ calibration for a new particle accelerator project, LHC," in *Proc. Eur. Conf. Power Electron. Appl.*, Sep. 2005, pp. 1–8.

[82] P. Arpaia, A. Ballarino, L. Bottura, and G. Montenero, "A cryogenic sensing element for measurement current transformers," *J. Instrum.*, vol. 9, no. 3, Mar. 2014, Art. no. P03011.

[83] *Nickel Iron and Cobalt Iron Cold Rolled Strips-Vibrotest Srl*. Accessed: Apr. 13, 2025. [Online]. Available: https://www.vibrotest.ro/sites/default/files/pictures/APERAM%201/Nickel%20Iron%20and%20Cobalt%20Iron%20Cold_Rolled_Strips.pdf

[84] M. T. Fard, J. He, H. Huang, and Y. Cao, "Aircraft distributed electric propulsion technologies—A review," *IEEE Trans. Transport. Electrific.*, vol. 8, no. 4, pp. 4067–4090, Dec. 2022.

[85] D. R. James, I. Sauers, A. R. Ellis, E. Tuncer, K. Tekletsadik, and D. W. Hazelton, "Breakdown and partial discharge measurements of some commonly used dielectric materials in liquid nitrogen for HTS applications," *IEEE Trans. Appl. Supercond.*, vol. 17, no. 2, pp. 1513–1516, Jun. 2007.

[86] C. I. Hill, S. Bozhko, T. Yang, P. Giangrande, and C. Gerada, "More electric aircraft electro-mechanical actuator regenerated power management," in *Proc. IEEE 24th Int. Symp. Ind. Electron. (ISIE)*, Buzios, Brazil, Jun. 2015, pp. 337–342.

[87] V. Madonna, P. Giangrande, and M. Galea, "Electrical power generation in aircraft: Review, challenges, and opportunities," *IEEE Trans. Transport. Electrific.*, vol. 4, no. 3, pp. 646–659, Sep. 2018.

[88] L. Andrade and C. Tenning, "Design of the boeing 777 electric system," in *Proc. IEEE Nat. Aerosp. Electron. Conf.@m_NAECON*, Jul. 1992, pp. 1281–1290.

[89] Y. Guo, Y. Xu, L. Liang, and Y. Liu, "Bonding wire fatigue life prediction of power module in thermal cycling test," in *Proc. 17th Int. Conf. Electron. Packag. Technol. (ICEPT)*, Wuhan, China, Aug. 2016, pp. 482–485, doi: 10.1109/ICEPT.2016.7583180.

[90] L. Xu, M. Wang, Y. Zhou, Z. Qian, and S. Liu, "Effect of silicone gel on the reliability of heavy aluminum wire bond for power module during thermal cycling test," in *Proc. IEEE 66th Electron. Compon. Technol. Conf. (ECTC)*, Las Vegas, NV, USA, May 2016, pp. 1005–1010, doi: 10.1109/ECTC.2016.172.

[91] U.-M. Choi, F. Blaabjerg, and S. Jørgensen, "Power cycling test methods for reliability assessment of power device modules in respect to temperature stress," *IEEE Trans. Power Electron.*, vol. 33, no. 3, pp. 2531–2551, Mar. 2018, doi: 10.1109/TPEL.2017.2690500.

[92] J. Lutz, "Power cycling–methods, measurement accuracy, comparability," in *Proc. 11th Int. Conf. Integr. Power Electron. Syst.*, Berlin, Germany, 2020, pp. 1–8.

[93] R. L. Patterson, A. Hammoud, and M. Elbuluk, "Assessment of electronics for cryogenic space exploration missions," *Cryogenics*, vol. 46, nos. 2–3, pp. 231–236, Feb. 2006, doi: 10.1016/j.cryogenics.2005.12.002.

[94] R. Patterson, R. Stone, and A. Hammoud, "Investigation of stepper motor controllers for ultra-low temperature environments," NASA Glenn Res. Center., Cleveland, OH, USA, Tech. Rep., Nov. 2002.

[95] D. Wikkerink, A. R. Mor, H. Polinder, and R. Ross, "Converter design for high temperature superconductive degaussing coils," *IEEE Access*, vol. 10, pp. 128656–128663, 2022.

[96] H. J. M. ter Brake and G. F. M. Wiegerinck, "Low-power cryocooler survey," *Cryogenics*, vol. 42, no. 11, pp. 705–718, Nov. 2002.

[97] H. Schefer, W.-R. Canders, J. Hoffmann, R. Mallwitz, and M. Henke, "Cryogenically-cooled power electronics for long-distance aircraft," *IEEE Access*, vol. 10, pp. 133279–133308, 2022.

[98] V. Ilardi, A. Dudarev, H. Silva, T. Koettig, L. N. Busch, P. B. de Sousa, and H. H. J. Ten Kate, "Conceptual design of the cryostat for a highly radiation transparent 2 T superconducting detector solenoid for FCC-ee^{+}," *IEEE Trans. Appl. Supercond.*, vol. 30, no. 4, pp. 1–5, Jun. 2020.

[99] B. Doshi, H. Xie, C. Zhou, R. Sidibomma, M. Meekins, C. Sborchia, K. Ioki, S. Tyge, A. K. Bhardwaj, and G. K. Gupta, "Design and manufacture of the ITER cryostat," in *Proc. IEEE 25th Symp. Fusion Eng. (SOFE)*, San Francisco, CA, USA, Jun. 2013, pp. 1–6.
[100] M. J. Gouge, J. A. Demko, M. L. Roden, J. F. Maguire, C. S. Weber, J. G. Weisend, J. Barclay, S. Breon, J. Demko, M. DiPirro, J. P. Kelley, P. Kittel, A. Klebaner, A. Zeller, M. Zagarola, S. Van Sciver, A. Rowe, J. Pfotenhauer, T. Peterson, and J. Lock, "Vacuum-insulated, flexible cryostats for long HTS cables: Requirements, status and prospects," *AIP Conf. Proc.*, vol. 985, no. 1, pp. 1343–1350, 2008, doi: 10.1063/1.2908492.
[101] T. H. Nicol, J. E. DiMarco, J. S. Kerby, T. M. Page, T. J. Peterson, and R. J. Rabehl, "LHC interaction region quadrupole cryostat production, alignment, and performance summary," *IEEE Trans. Appl. Supercond.*, vol. 14, no. 2, pp. 247–250, Jun. 2004.
[102] (2024). *Liquid Hydrogen As a Potential Low-carbon Fuel for Aviation*. Accessed: May 21, 2024. [Online]. Available: https://www.iata.org/contentassets/d13875e9ed784f75bac90f000760e998/fact_sheet7-hydrogen-fact-sheet_072020.pdf
[103] M. G. Alfarizi, F. Ustolin, J. Vatn, S. Yin, and N. Paltrinieri, "Towards accident prevention on liquid hydrogen: A data-driven approach for releases prediction," *Rel. Eng. Syst. Saf.*, vol. 236, Aug. 2023, Art. no. 109276, doi: 10.1016/j.ress.2023.109276.
[104] Universal Hydrogen. *Universal Hydrogen Receives G-1 From the FAA, Marking Key Step in Establishing the Certification Standards for Hydrogen-Powered Flight*. Accessed: May 21, 2024. [Online]. Available: https://hydrogen.aero/press-releases/universal-hydrogen-receives-g-1-from-the-faa-marking-key-step-in-establishing-the-certification-standards-for-hydrogen-powered-flight/

ABDELRAHMAN ELWAKEEL (Member, IEEE) received the B.Sc. and M.Sc. degrees from Alexandria University, Egypt, and the Ph.D. degree from the University of Strathclyde, Glasgow, Scotland, U.K. He has worked in the industry of design engineering for three years. He is currently a Research Associate at the University of Strathclyde. His research interests include cryogenic power electronics, transportation electrification, and machine learning.

YUCHUAN LIAO (Graduate Student Member, IEEE) received the master's degree from the University of Stuttgart, Germany. He is currently pursuing the Ph.D. degree with the Applied Superconducting Research Group, University of Strathclyde, Glasgow. His research interest includes the power electronics at cryogenic temperature, especially the GaN transistors and corresponding converters.

YUDI XIAO (Member, IEEE) received the B.Sc. and M.Sc. degrees in power electronics from Fuzhou University, Fuzhou, China, in 2015 and 2018, respectively, and the Ph.D. degree from the Technical University of Denmark, Kongens Lyngby, Denmark, in 2022. He was an Industrial Ph.D. Student and an Electronics Engineer with Welltec A/S, Allerød, Denmark, from 2018 to 2023. He is currently a Research Associate at the University of Strathclyde. His research interests include harsh environment power electronics and high-frequency magnetic technologies in power electronics.

RAFAEL PEÑA ALZOLA (Senior Member, IEEE) received the combined Licentiate and M.Sc. degree in industrial engineering from the University of the Basque Country, Bilbao, Spain, in 2001, and the Ph.D. degree in electrical engineering from the National University for Distance Learning, Madrid, Spain, in 2011. He has worked as an Electrical Engineer for several companies in Spain. From September 2012 to July 2013, he was a Guest Postdoctoral Fellow with the Department of Energy Technology, Aalborg University, Aalborg, Denmark. From August 2014 to December 2016, he was a Postdoctoral Research Fellow with the Department of Electrical and Computer Engineering, The University of British Columbia, Vancouver, BC, Canada. From January 2017 to May 2017, he was with the University of Alcala, Madrid, for a short-term industrial collaboration. Since June 2017, he has been a Research Fellow with the Rolls Royce University Technology Centre, University of Strathclyde, Glasgow, U.K. His research interests include energy storage, LCL filters, solid-state transformers, power electronics for hybrid electric aircraft, and innovative control techniques for power converters.

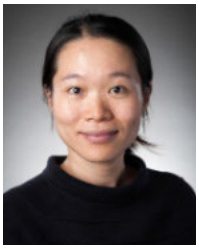

MIN ZHANG (Senior Member, IEEE) received the bachelor's and master's degrees in electrical engineering from Tsinghua University, China, and the Ph.D. degree in engineering from the University of Cambridge, U.K. She spent a year as a Junior Research Fellow at the Newnham College, University of Cambridge, and then joined the University of Bath as a Lecturer. In 2018, she joined the University of Strathclyde as a Reader. Her research interests include the application of high-temperature superconductors in power system transmission, renewable generation, and electric transportation. She is a Research Fellow of the Royal Academy of Engineering.

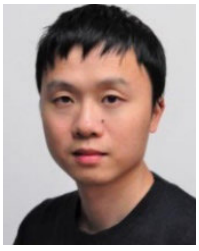

WEIJIA YUAN (Senior Member, IEEE) received the bachelor's degree from Tsinghua University, in 2006, and the Ph.D. degree from the University of Cambridge, in 2010. Then, he became a Research Associate with the Engineering Department and a Junior Research Fellow at the Wolfson College, University of Cambridge, from 2010 to 2011. In 2011, he joined the University of Bath, U.K., as a Lecturer/Assistant Professor, where he was later promoted to a Reader/Associate Professor, in 2016. In 2018, he joined the University of Strathclyde, U.K., as a Professor.